



RESEARCH ARTICLE

10.1029/2017JA025153

Interhemispheric Survey of Polar Cap Aurora

J. A. Reidy^{1,2} , R. C. Fear¹ , D. K. Whiter¹ , B. Lanchester¹ , A. J. Kavanagh^{2,3} , S. E. Milan^{4,5} , J. A. Carter⁴ , L. J. Paxton⁶ , and Y. Zhang⁶

Key Points:

- We present a statistical survey of the interhemispheric nature and particle precipitation of polar cap auroras imaged from low Earth orbit
- We find evidence for polar cap arcs which form on open field lines, and others which form on closed field lines
- We find a case of a of nonconjugate theta aurora that are inconsistent with a closed field line model

Supporting Information:

- Supporting Information S1

Correspondence to:

J. Reidy,
jr10g11@soton.ac.uk

Citation:

Reidy, J., Fear, R. C., Whiter, D., Lanchester, B. S., Kavanagh, A. J., Milan, S. E., et al. (2018). Interhemispheric survey of polar cap aurora, *Journal of Geophysical Research: Space Physics*, 123, 7283–7306. <https://doi.org/10.1029/2017JA025153>

Received 4 JAN 2018

Accepted 13 JUL 2018

Accepted article online 20 JUL 2018

Published online 4 SEP 2018

©2018. The Authors.

This is an open access article under the terms of the Creative Commons Attribution License, which permits use, distribution and reproduction in any medium, provided the original work is properly cited.

¹Department of Physics and Astronomy, University of Southampton, Southampton, UK, ²British Antarctic Survey, Natural Environment Research Council, Cambridge, UK, ³Visiting Scientist at the Rutherford Appleton Laboratory, Science and Technology Facilities Council, Didcot, UK, ⁴Department of Physics and Astronomy, University of Leicester, Leicester, UK, ⁵Birkeland Centre for Space Science, University of Bergen, Norway, ⁶The Johns Hopkins University Applied Physics Laboratory, Laurel, MD, USA

Abstract This study investigates the interhemispheric nature of polar cap auroras via ultraviolet imaging, combined with particle data, to determine whether they occur on open or closed field lines. Data from the SSUSI (Special Sensor Ultraviolet Spectrographic Imager) instrument on board the DMSP (Defence Meteorological Satellite Program) spacecraft are examined. The DMSP spacecraft are in 90-min orbits; hence, images of each hemisphere are separated by 45 min providing a good opportunity for interhemispheric study. 21 polar cap arc (PCA) events are recorded in December 2015 which have particle data from the SSJ/4 particle spectrometer associated with an arc in at least one hemisphere. Nine events are found to contain "arcs" consistent with a closed field line mechanism, that is, arcs associated with an ion signature present in both hemispheres. Six events contained arcs that were consistent with an "open field line" mechanism, that is, they were associated with electron-only precipitation. Events containing arcs that were not consistent with either of these expectations are also explored, including an example of a "non-conjugate" theta aurora and an interesting example of auroral morphology similar to a PCA which is associated with a geomagnetic storm. Seasonal effects are also investigated through a statistical analysis of PCAs over 4 months in 2015. It is found that PCAs are visible in the SSUSI data at least 20% of the time and that it is likely some are missed due to the spacecraft field of view and poor sensitivity in the summer hemisphere due to increased solar illumination.

1. Introduction

Polar cap arcs (PCAs), also known as high latitude or Sun-aligned arcs, are auroras occurring within the typically "dark" polar cap and have been studied for over a century (Mawson, 1916). These arcs connect to the nightside of the oval (sometimes in the midnight sector, and sometimes at dawn/dusk). On occasion these arcs have been observed to connect the day and nightside oval, known as "theta" aurora (Frank et al., 1982). PCAs have been found to be correlated with northward interplanetary magnetic field (IMF) and periods of low magnetospheric activity (Berkey et al., 1976; Gussenhoven, 1982). Many different mechanisms have been put forward to explain these arcs, some of which are reviewed in Zhu et al. (1997), Fear and Milan (2012a), and references therein. Some of these mechanisms predict that the arcs form on open field lines and others on closed field lines, an issue which is still under debate. This paper will discuss arcs occurring on open and closed field lines. Reidy et al. (2017) presented a case study arguing that PCAs with these two different topologies could occur simultaneously.

The occurrence of PCAs is naturally associated with the presence of plasma precipitation in the polar cap. Winningham and Heikkila (1974) first classified precipitation in the polar cap depending on how structured and energetic it appeared. Their first classification was of a uniform weak (~100 eV) electron-only precipitation seen over the entire polar cap, and they suggested that it may be present at all times. This type of polar cap precipitation is known as polar rain and has subsequently been found to consist of solar wind electrons that enter the magnetosphere on open field lines (e.g., Baker et al., 1986). The second classification of polar cap particle precipitation from Winningham and Heikkila (1974) was a localized flux of higher-energy electrons (~1 keV), termed *polar showers*, that could intensify during periods of geomagnetic activity. Polar showers are known to occur during northward IMF (Hardy, 1984; Hardy et al., 1986; Shinohara & Kokubun, 1996). Shinohara and Kokubun (1996) discussed two different types of polar showers—one with accompanying

ion fluxes and one without. The type without an ion signature was found to follow polar rain statistics, for example, a favored hemisphere determined by the IMF B_x component and a dawn-dusk gradient determined by IMF B_y (Meng & Kroehl, 1977; Yeager & Frank, 1976) and hence was suggested to be occurring on open field lines. The polar showers occurring with ion precipitation did not show dependences on the IMF B_x or B_y components and were generally more energetic than the type without ions. The intensity of these showers led Shinohara and Kokubun (1996) to suggest they were occurring on closed field lines. An associated phenomenon is the presence of Polar Cap Ion Beams (PCIBs), which occur at higher altitudes, and which are regarded as the higher altitude counterpart of accelerated electron signatures at lower altitudes (where electrostatic potential structures accelerate ionospheric ions upward and magnetospheric electrons downward). In a statistical study using Cluster data, Maggiolo et al. (2011) found upward-directed PCIBs to have similar properties to PCAs, suggesting that they were both signatures of the same phenomenon. Furthermore, they found 40% of PCIBs to be associated with an isotropic ion population (suggestive of a closed field line topology) but in the remaining 60% the isotropic component was absent. Additionally, during northward IMF, the cusp spot is driven by lobe reconnection and hence located just poleward of the auroral oval (e.g., Milan et al., 2000a). Cusp precipitation (on open field lines) is known to contain ions (e.g., Frey et al., 2003; Yeoman et al., 1997); and therefore, although ion precipitation in the polar cap is usually indicative of closed field lines, care should be taken closer to the sunward edge of the polar cap, where ion precipitation may be associated with the cusp spot and hence may be occurring on open field lines.

It has long been suggested that accelerated polar rain (meaning polar showers without accompanying ion fluxes) could be the cause of the Sun-aligned PCAs. For example, Hardy et al. (1982) reported PCAs embedded within polar rain. Carlson and Cowley (2005) argued that any mechanism that drives shear flows across open field lines, that is, those in the lobes, could generate subvisual PCAs consistent with accelerated polar rain on open field lines. Newell et al. (2009) proposed three distinct types of polar cap aurora, depending on their plasma signatures: first, a common, low intensity arc occurring as a result of accelerated polar rain (i.e., consistent with Carlson & Cowley, 2005) that is not associated with ion precipitation; second, a slightly more intense arc that is associated with ion precipitation and occurs adjacent to the auroral oval; and the third type discussed by Newell et al. (2009) is an arc completely detached from the main auroral oval (when viewed on a dawn-dusk pass, i.e., well within the polar cap) that is associated with ion precipitation and can occur for some hours. Newell et al. (2009) consider the first two types of PCA to be much more frequent than the third. In fact, Carlson and Cowley (2005) suggest that the polar rain accelerated arcs could be present in the polar cap almost half of the time, that is, almost all of the time when the IMF is northward. In a ground-based statistical study, Hosokawa et al. (2011) found weak PCAs to occur at least 40% of the time.

Large-scale PCAs were discovered using UV satellite images (Frank et al., 1982, 1986). These arcs were found to be associated with a plasma signature, including an ion signature, of similar energy to the main auroral oval, hence suggesting they too occurred on closed field lines (Frank et al., 1986); these arcs are sometimes known as transpolar arcs (TPAs). In this paper, we use *PCA* as a general term for auroras occurring within the polar cap which describes both TPAs, typically thought to be on closed field lines, and lower energy arcs on open field lines (e.g., Carlson & Cowley, 2005). The term theta aurora is also used synonymously for TPAs. Milan et al. (2005) proposed a mechanism to explain how these closed field lines are in the typically "open" polar cap. They suggest that tail reconnection during northward IMF, and under the influence of an IMF B_y component, causes newly closed flux to become trapped in the tail. Predictions from this mechanism have been verified by Fear and Milan (2012a), who explored the relation between the position where arcs formed in the polar cap and the IMF B_y component, and Fear and Milan (2012b), who found statistical evidence for reconnection-induced flows in the ionosphere before the formation of the TPAs. Furthermore, several recent case studies have also provided evidence in support of this mechanism (e.g., Carter et al., 2017; Fear et al., 2014; Goudarzi et al., 2008).

One issue surrounding mechanisms that put PCAs on closed field lines is the so called non-conjugate theta aurora. Any mechanism that puts PCAs on closed field lines predicts that they will occur in both hemispheres simultaneously. The first example of a TPA observed in both hemispheres simultaneously was presented by Craven et al. (1991) using images from the Dynamics Explorer 1 and Viking satellites. However, two events were presented by Østgaard et al. (2003) with simultaneous observations of the auroral regions in both hemispheres with a TPA observed in only one hemisphere. Simultaneous low-altitude particle data were also avail-

able for these events, and it was found that both TPAs had an ion signature comparable to the main oval, which the authors suggested was indicative of their occurring on closed field lines; however, no ions were detected in the opposite hemispheres. Conversely, Østgaard et al. (2003) interpret these arcs as being formed as a result of lobe reconnection, implicitly suggesting that they are occurring on open field lines. One further observation of a non-conjugate theta aurora was presented in Østgaard et al. (2007). Østgaard et al. (2003) suggest that a possible explanation for the observations is the difference in conductivity between sunlit and nonsunlit hemispheres, which would lead to the suppression of the arc in the summer hemisphere. They also argue that differences in the polarity of the IMF B_x component could be the cause, as lobe reconnection is favored in one hemisphere depending on IMF B_x . Fear and Milan (2012a) briefly discussed a possible interpretation based on the Milan et al. (2005) mechanism, suggesting that the hemisphere without the PCA may have experienced lobe reconnection (which, in the Milan et al., 2005, mechanism, drives the motion of TPAs) and hence the arc in that hemisphere could have moved and become indistinguishable from the main oval before the first observations in that hemisphere were available. However, this issue is still unresolved and hence further exploration is warranted.

This study uses particle data in conjunction with a low-altitude UV imager with near-simultaneous observations to investigate these different mechanisms, with the motivation that the magnetic field line topology of the PCAs may be determined by their particle precipitation and hemispheric nature. New capabilities, including low-altitude auroral imagery from the Special Sensor Ultraviolet Spectrographic Imager (SSUSI) instruments on board several of the Defense Meteorological Satellite Program (DMSP) spacecraft, have led to a renewal of interest in interhemispheric observations of PCAs and associated plasma signatures. Carter et al. (2017) reported a simultaneous observation of PCAs occurring in both hemispheres using data from SSUSI and Imager for Magnetopause-to-Aurora Global Exploration (IMAGE). Using the particle data from the DMSP SSJ/4 spectrometer they showed the arcs to be associated with ion precipitation, consistent with formation on closed field lines. Xing et al. (2018) presented a similar observation with a conjugate PCA associated with ion precipitation in the DMSP particle data that was hence also consistent with a closed field line mechanism. DMSP particle data were also published in association with a large-scale PCA in Fear et al. (2014). Their observations showed an arc associated with an ion signature that was consistent with the closed field line tail reconnection mechanism suggested by Milan et al. (2005). Cumnock et al. (2009) also used SSJ/4 particle data to examine the structure within large-scale PCAs, finding a small number of them to be composed of multiple distinct thin arcs associated with ion signatures. On the other hand, Reidy et al. (2017) presented observations from SSUSI of an arc occurring only in one hemisphere that was found to be associated with an electron-only signature in the DMSP SSJ/4 particle data; this arc was seen to be occurring simultaneously with an arc found to be on closed field lines on the other side of the northern hemisphere polar cap. Furthermore, the position of the electron-only arc within the polar cap and the hemisphere in which it occurred were consistent with the IMF preferences found for polar rain. It was hence determined that this arc was an example of a PCA occurring on open field lines, formed by accelerated polar rain.

Previous PCA surveys have shown different occurrence rates for PCAs. A ground-based survey by Valladares et al. (1994) using all-sky imagers in Qaanaaq, Greenland, located near to the magnetic north pole, found PCAs to be occurring at least 40% of the time, whereas Kullen et al. (2002) found an occurrence of at least 10% of the time using data from Polar UV. This possible difference in ground-based to spacecraft PCA surveys is reflected in the 130 PCAs identified by Fear and Milan (2012a) in IMAGE data over a 5-year interval compared to the 743 arcs identified over 5 years of all-sky imager data at Resolute Bay, Canada, by Hosokawa et al. (2011), although these figures cannot be directly compared due to different observational coverage (e.g., spacecraft orbital variation for the IMAGE data and the requirement for darkness/absence of cloud coverage in the all-sky camera observations). The difference in PCA occurrence could be due to the different types of PCAs, with the lower energy arcs dominating the ground-based studies and perhaps being missed by the UV imagers that see only the brighter larger scale events.

This study aims to investigate PCA occurrence by surveying 4 months of low-altitude UV auroral imager data during 2015. Furthermore, PCA formation mechanisms are considered by comparing the UV auroral images in each hemisphere and using particle data to investigate the precipitation associated with these arcs. The instrumentation used in this study is described in section 2. Section 3 discusses the PCA events recorded in

December 2015 in conjunction with the corresponding particle data. The events are separated depending on whether they were observed in one or both hemispheres. In section 4, the seasonal effects on the occurrence of PCAs are investigated using 4 months of SSUSI data in 2015. Lastly, a discussion and conclusions are given in sections 5 and 6.

2. Instrumentation

In order to identify PCAs, this study makes use of three SSUSI instruments on board DMSP spacecraft F16, F17, and F18 (Paxton et al., 2002). The DMSP spacecraft are in 90-min Sun-synchronous orbits at an altitude of approximately 850 km, hence images of each hemisphere are available 45 min apart. There is further opportunity for near-simultaneous interhemispheric observations when using all three spacecraft due to their overlapping orbits. When over the polar regions, SSUSI scans antisunward along its orbit, building up an image of a swath of the auroral region over 20 min. These images are produced at five different wavelengths simultaneously. This study uses the Lyman-Birge Hopfield long band, 165–180 nm, which is comparable to wavelengths used for previous PCA observations from the IMAGE satellite (e.g., Fear et al., 2014, 2015; Milan et al., 2005); this emission is mainly from precipitating electrons.

In conjunction with the SSUSI images, data are obtained from the SSJ/4 particle detector also on board the DMSP spacecraft. These provide measurements of the electron and ion energy spectra along the track of the spacecraft. In one case, we provide supporting observations of the global field-aligned current systems inferred from the AMPERE data set (Anderson et al., 2000, 2014; Coxon et al., 2014a, 2014b, 2016, 2018; Waters et al., 2001).

Data from OMNI (King & Papitashvili, 2005) and Artemis 1 (Auster et al., 2008) are also obtained to evaluate the IMF conditions during the PCA events.

3. Observations

Data from December 2015 were obtained from the SSUSI instruments on DMSP spacecraft F16, F17, and F18. This was an interval when data from all three spacecraft were available and coincided with an instrument campaign ran by the University of Southampton for the Auroral Structure and Kinetics (ASK) instrument, a multimonochromatic imager located near Longyearbyen, Svalbard (Ashrafi, 2007; Dahlgren et al., 2008). Over that month, 43 polar cap aurora events were identified in the SSUSI data. These events are defined by the presence of PCAs in the SSUSI images; SSUSI images with more than one arc are counted as one event.

Once identified, the events were classified using the SSUSI images in both hemispheres. To be classified as a both hemisphere event, the arc had to be visible in two subsequent images, one from each hemisphere. As discussed later, this classification does not necessarily imply conjugacy, as independent open field line arcs could form in both hemispheres simultaneously. To be classified as a "one hemisphere" event, the arc had to appear in one SSUSI image, then be absent in the next available images for all spacecraft in the opposite hemisphere, but then still be visible in the subsequent images of the original hemisphere. If an arc was seen in one image, not in the following hemispheric images and then not in the next images of the original hemisphere, it was left unclassified. This is because the arc was not visible in the SSUSI images long enough for its hemispheric nature to be determined. Events where the SSUSI field of view was obstructed in one hemisphere or where the data quality was not good enough to distinguish the main auroral oval were left unclassified.

Out of the 43 events identified in December 2015, 19 were seen in both hemispheres, 8 in one hemisphere only, and 16 were left unclassified. In this paper, we consider only the events that could be classified as one hemisphere or both hemisphere and that had particle data from the SSJ/4 instruments on board the DMSP spacecraft. All 19 both hemisphere and 2 of the 8 one hemisphere events had particle data. Figure 1 shows the IMF B_y and B_z components averaged over the event duration for these 21 events. The event duration is given by the start and end times of the first and last SSUSI images, respectively, containing PCAs. From Figure 1, it can be seen that most of the events occurred during northward IMF or B_z close to zero. The color coding is discussed below in sections 3.1 and 3.2. The filled-in circles correspond to both hemisphere events, and the open circles represent one hemisphere events.

Data from the particle spectrometer on board the DMSP spacecraft were obtained for events when the spacecraft track crossed the arc and were used to classify whether each event corresponded to open or closed field

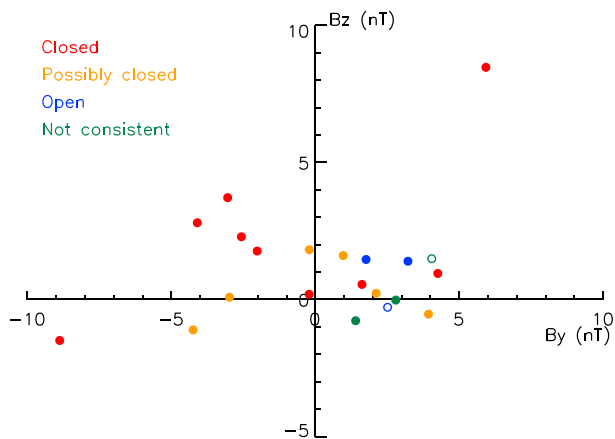


Figure 1. Interplanetary magnetic field B_y and B_z components averaged over each of the 22 events identified. The colors denote the possible classifications with filled circles for both hemisphere events and open circles for one hemisphere events.

lines. If arcs are associated with an ion signature and seen in both hemispheres, then they are consistent with a closed field line formation mechanism (e.g., Carter et al., 2017; Xing et al., 2018). If the arcs are associated with an electron-only signature, then they are consistent with an open field line mechanism (Newell et al., 2009; Reidy et al., 2017), whether they are seen in one or both hemispheres. Ion and electron signatures are identified when the summed energy flux of the high energy particles is above a certain threshold. For an arc to be classified as having an ion signature, we required both the summed ion and electron fluxes to be above a certain value; this was required in an attempt to avoid associating cusp precipitation (which occurs on open field lines but may contain ions; Frey et al., 2003) with the PCAs, particularly on DMSP passes which orbit close to the dayside aurora. Hence, in this paper, when we refer to an arc having an *ion signature*, we technically mean an ion and an electron signature. For an electron-only signature, we required the summed electron flux to be above a certain threshold and the summed ion flux to be below a threshold. We found it was not possible to set a single threshold that could be used uniformly for all events, which would identify all plasma signatures

in all events without also identifying "noise" in the spectrograms of some other events. Therefore, the threshold was adjusted in some cases based on a manual examination of the spectrograms, the auroral images, and the summed flux time series. Full details of the method used to identify the particle signatures are given in supporting information S1.

3.1. Events Occurring in Both Hemispheres

Table 1 lists the 19 events identified as occurring in the polar caps of both hemispheres simultaneously. In all 19 cases, there was a pass by a DMSP satellite over the PCA in at least one hemisphere on at least one

Table 1
Events Identified as Occurring in Both Hemispheres in SSUSI

Event num.	Start time (UT)	End time	NH ion sig.	SH ion sig.	Classification
03	02 Dec 2015 22:21	03 Dec 2015 01:17	y	y	Closed
04	03 Dec 2015 14:36	03 Dec 2015 16:36	y	y	Not consistent
06	03 Dec 2015 23:59	04 Dec 2015 01:04		y	Possibly closed
07	04 Dec 2015 08:36	04 Dec 2015 13:14	y	y	Closed
08	04 Dec 2015 16:11	04 Dec 2015 21:26	y		Possibly closed
10	06 Dec 2015 13:09	06 Dec 2015 16:09	y		Possibly closed
11	06 Dec 2015 17:22	06 Dec 2015 18:38	n	n	Open
14	08 Dec 2015 11:06	08 Dec 2015 12:59	n	y	Not consistent
15	08 Dec 2015 14:25	08 Dec 2015 15:18	n	n	Open
22	14 Dec 2015 17:21	14 Dec 2015 20:55	y	y	Not PCA
23	15 Dec 2015 12:55	15 Dec 2015 14:11	y		Possibly closed
24	15 Dec 2015 17:08	15 Dec 2015 20:45	y	y	Both closed and open observed simultaneously
26	16 Dec 2015 18:36	16 Dec 2015 23:56	y	y	Closed
31	22 Dec 2015 13:04	22 Dec 2015 18:16	y	y	Closed
35	25 Dec 2015 18:18	25 Dec 2015 22:09	y	y	Closed
38	27 Dec 2015 01:02	27 Dec 2015 01:20		y	Possibly closed
39	27 Dec 2015 14:28	27 Dec 2015 18:18	y	y	Closed
40	27 Dec 2015 22:01	28 Dec 2015 00:49		y	Possibly closed
43	31 Dec 2015 16:06	31 Dec 2015 18:15	y and n	y	Closed

Note. Event times are extracted from the SSUSI images whereby the start and end times are recorded when the DMSP spacecraft crosses 70° magnetic latitude. All arcs that intersected the DMSP footprint have an electron signature. The arcs with an accompanying ion signature are marked by y, electron-only arcs n. The column is left blank if the DMSP footprint does not intersect the arc. The classification of the arc, that is, whether it is consistent with an open or closed field line mechanism, is indicated in the last column, with the same categories as in Figure 1. PCA = polar cap arc; DMSP = Defense Meteorological Satellite Program.

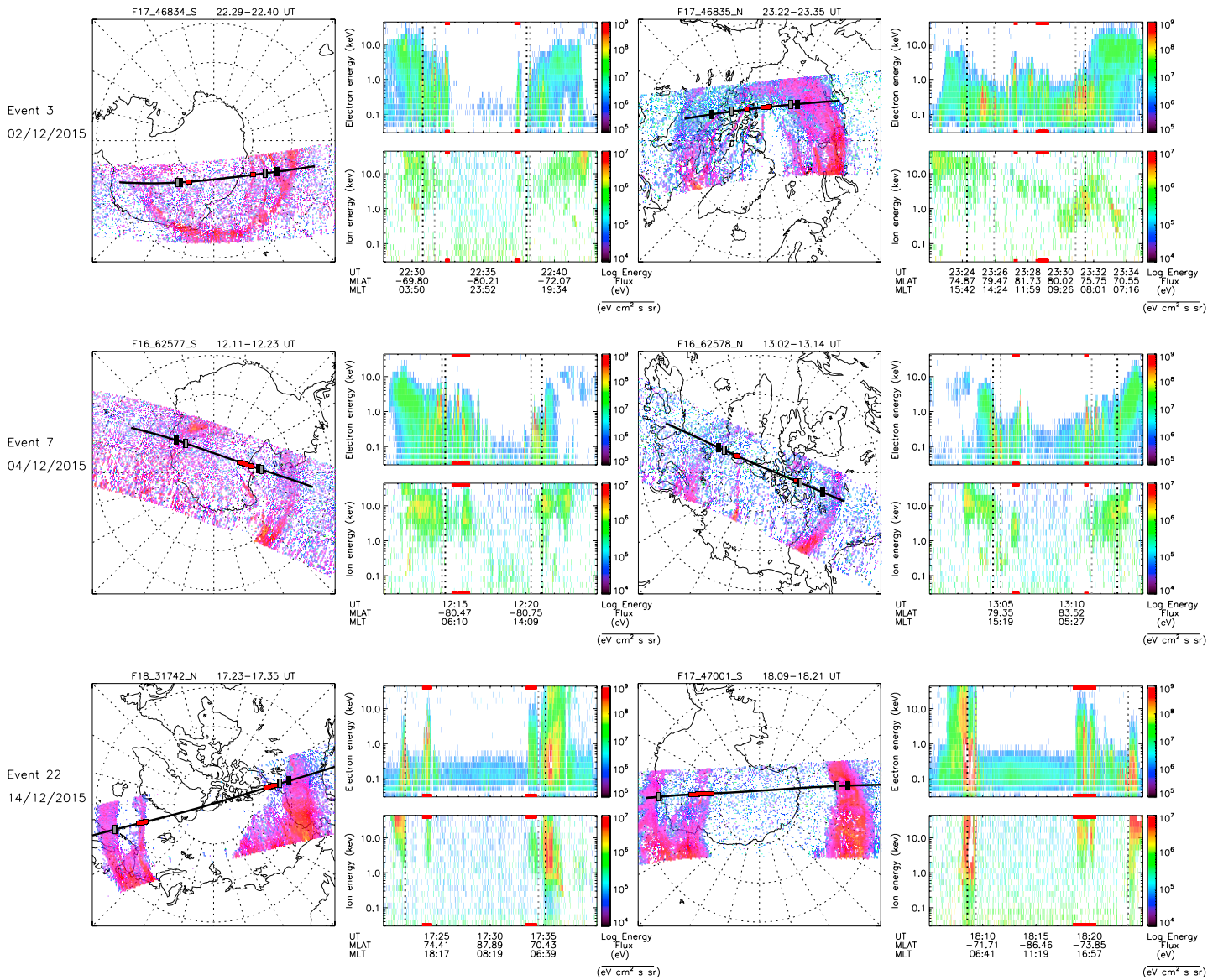


Figure 2. Summary images for arcs with polar cap arcs in both hemispheres associated with ion signatures. Each row represents an event with a summary SSUI image from each hemisphere during the event and the corresponding DMSP SSJ/4 particle data. The black line on the DMSP data is the footprint of the DMSP. Ion signatures are indicated in red, electron-only signatures are indicated in orange—Continued overleaf.

orbit and hence particle data for these arcs have been obtained. As these arcs are seen to be occurring in both hemispheres, our initial expectation would be for them to be consistent with a closed field line formation mechanism, and hence we expect to see an electron and an ion signature associated with these arcs. The fourth and fifth columns of Table 1 list which arcs had an ion signature in either or both hemispheres. These columns are left blank for events when the arc does not intersect the DMSP track. All arcs were associated with an electron signature on the passes which intersected the arc. It can be seen that (a) nine of the events contain arcs with an ion signature in both hemispheres, (b) two have electron-only signatures in both hemispheres, (c) two have an ion signature in one hemisphere and an electron-only signature in the other, and (d) six have an ion signature in one hemisphere but the arc in the opposite hemisphere did not intersect the DMSP footprint and hence no particle data could be obtained for those arcs. We discuss each of these groups below by classification, which is indicated in the last column of Table 1 and also indicated in Figure 1, but at this point note that (a) and possibly (d) are consistent with our expectations (i.e., with closed field lines, given that they are present in both hemispheres), whereas (b) and (c) are not. Events in group (b) are potentially consistent with independent simultaneous open field line arcs in the two hemispheres. Note that Events 22 and

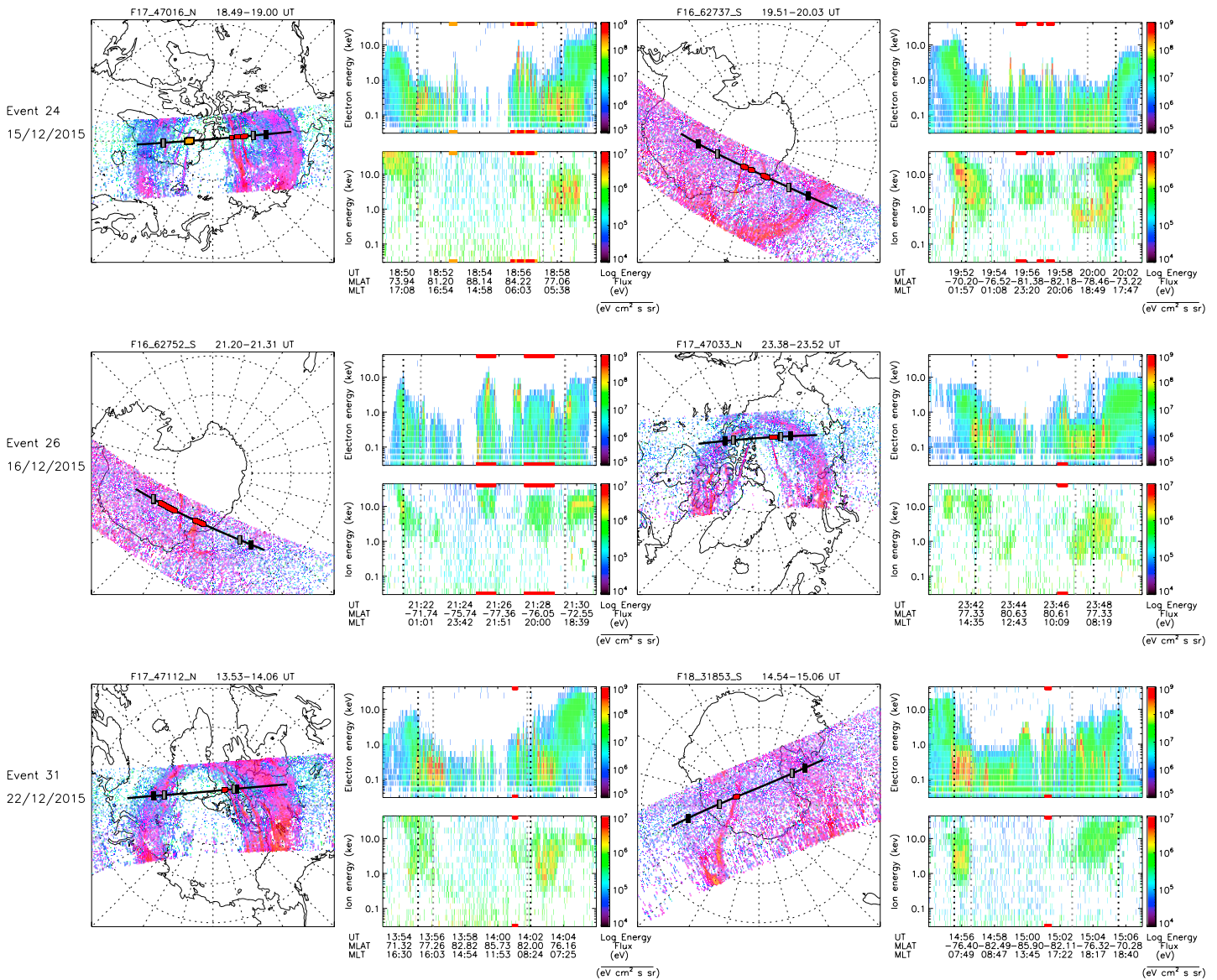


Figure 2. (continued)

24 contain auroral structures initially identified as PCAs, associated with ion signatures in both hemispheres and are hence included in group (a) but are classified differently as *Not PCA* and *Both open and closed observed simultaneously*. This will be addressed in sections 3.1.1 and 3.1.2, respectively.

3.1.1. (a) Consistent with a Closed Field Line Mechanism

Figure 2 shows summary images for all the events with a PCA associated with ion precipitation in both hemispheres. Each row consists of four figures corresponding to a single event. For each event, the clearest SSUSI images (i.e., the images where the PCA is most visible) and the corresponding SSJ/4 spectrograms are chosen from each hemisphere. The SSUSI images are projected onto magnetic local time grids, and the southern hemisphere images have been flipped across the noon-midnight meridian for ease of comparison with the northern hemisphere, such that noon is to the top of each image and dawn is always to the right. This means the DMSP track on the southern hemisphere SSUSI images is in the opposite direction (i.e., from right to left) to the northern hemisphere passes and hence features are mirrored in the southern hemisphere SSUSI and SSJ/4 images. Ion and electron-only signatures, meaning the presence of electron and ion fluxes with energies greater than approximately 1 keV, are identified from the DMSP SSJ/4 data. These are shown on the ion and electron spectrograms and on the track of the DMSP spacecraft (black line) in the SSUSI images in red, for arcs

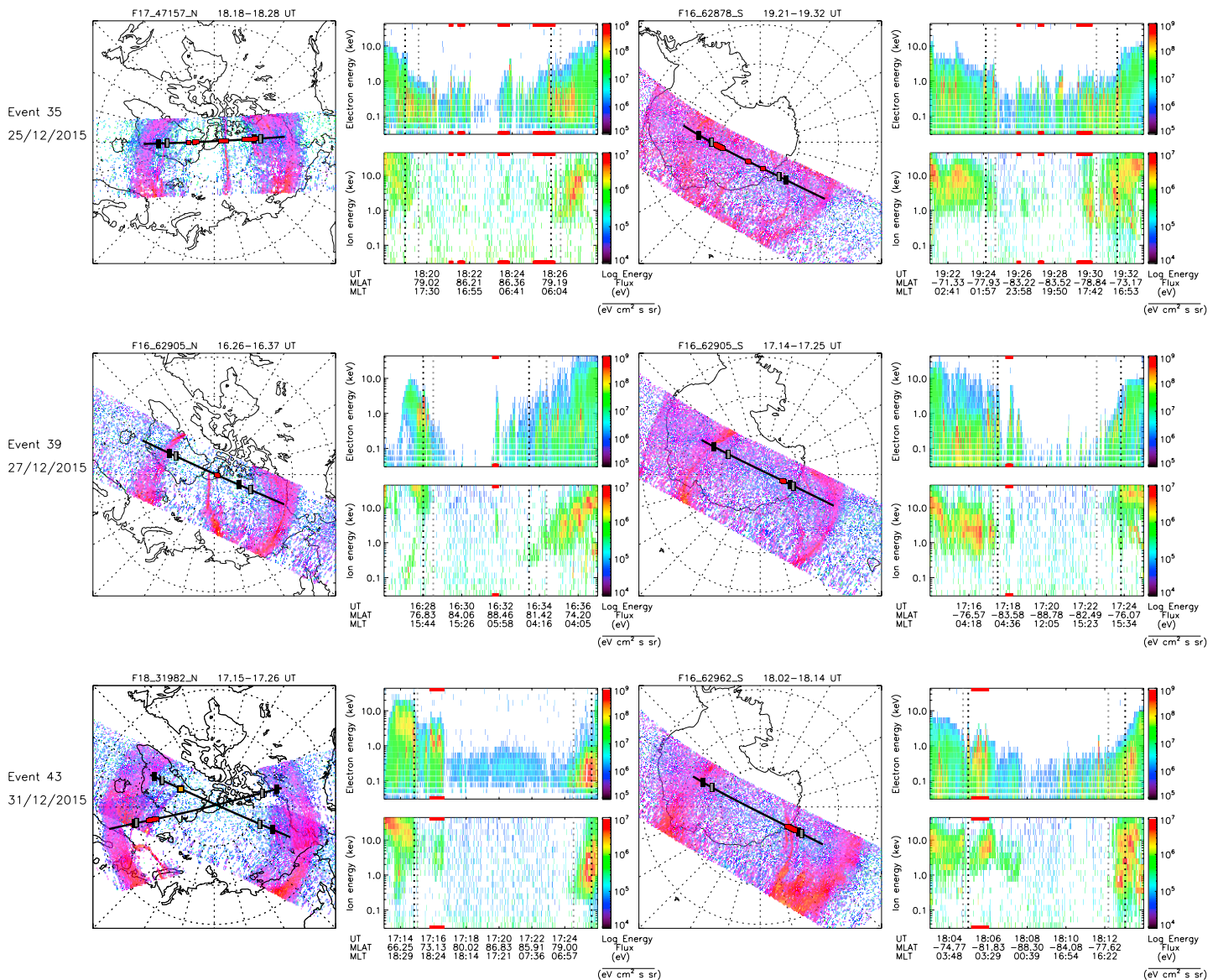


Figure 2. (continued)

associated with ion precipitation, and orange, for arcs associated with electron-only precipitation (e.g., Event 24, row 4, shows an example of both). An estimated position for the poleward boundary of the auroral oval is also indicated for each event (dashed vertical lines on the particle spectrograms and small vertical lines on the DMSP track on the SSUSI images—grey for the ion boundary and black for the electrons). These boundaries are defined as where there is a significant drop in the high energy particle fluxes poleward of the auroral oval (Newell et al., 1996). Full details of the method used to define these boundaries are given in supplementary material.

All of the events shown in Figure 2 contain arcs associated with an ion signature in both hemispheres and are hence consistent with formation on closed field lines. These arcs are represented in Figure 1 by the red filled circles. In each of the particle spectrograms in Figure 2, energetic signatures in both the electrons and ions can be seen corresponding to the PCAs, indicated in red. High energy electron and ion precipitation is detected in either side of the PCA as the spacecraft passes through the main auroral oval (e.g., Event 3, top row of Figure 2). In some spectrograms, low energy *uniform* precipitation can be seen between the oval signatures in the electron spectrograms (e.g., Event 22, third row of Figure 2); this type of signature is typical of what is expected for polar rain (e.g., Gussenhoven et al., 1984). Note that the DMSP spacecraft passes close to the

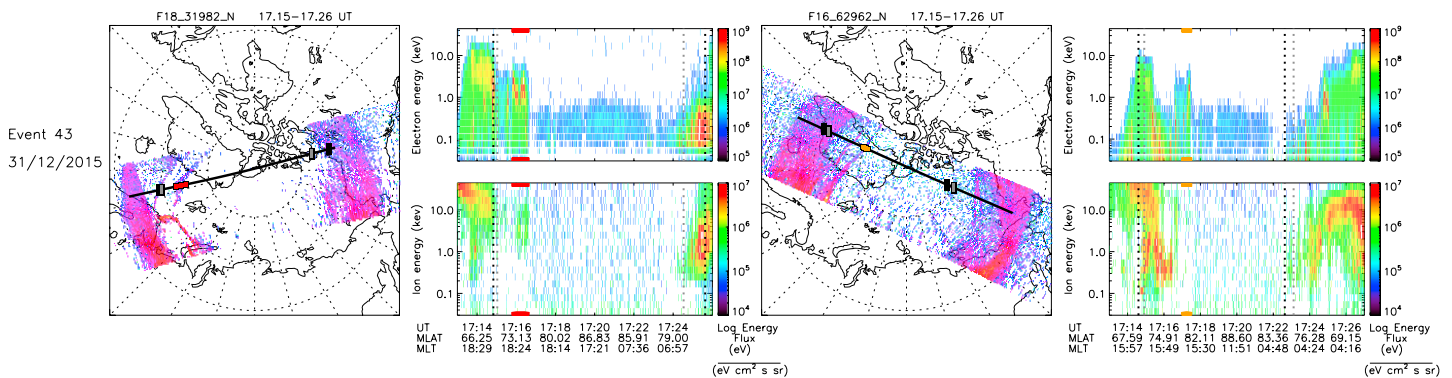


Figure 3. The SSUSI and corresponding SSJ/4 data for both northern hemisphere passes shown in Figure 2 for Event 43.

dayside in the northern hemisphere in Events 3 and 26 (first and fifth row of Figure 2). As cusp precipitation (on open field lines) can include ions, the SSUSI images were also examined in the Lyman-alpha channel (not shown). No obvious evidence of a cusp spot could be seen for either event, although it is possible that the particle flux was not high enough to generate an auroral signature for the cusp.

The northern hemisphere summary image for Event 43 (bottom row of Figure 2) consists of two SSUSI images overlaid. The main image (and the electron and ion spectrograms shown) are taken from the DMSP F18 spacecraft; the pass occurred between 17:15 and 17:26 UT and the corresponding footprint is indicated in the SSUSI images by the solid black line. The background image is from the DMSP F16 spacecraft, between 17:15 and 17:25 UT, and is indicated by the dashed DMSP footprint. It can be seen that despite the simultaneity of the two passes, the two DMSP SSJ/4 instruments detect different signatures associated with the same arc, with an ion signature observed by the F18 instrument (red) and an electron-only signature by F16 (orange). Figure 3 shows the SSUSI image and DMSP particle data from both spacecraft passes separately. This observation presents some interesting issues and will be examined further in section 5.

Figure 4 shows the IMF conditions for all the events shown in Figure 2, from 2 hr before the start time of the event. Each row corresponds to an event from Figure 2. The SSUSI passes in each hemisphere are indicated throughout the event with boxes; passes where a PCA was observed are shown as solid boxes. Passes where no PCA was observed are shown by a dashed box, in these cases it is likely that the PCA was not observed due to issues with the SSUSI field of view or noise in the image such that no arc could easily be discerned. In some cases the sensitivities of the spacecraft differed and hence PCAs were not observed in all three DMSP passes; this issue will be discussed further in section 4. From Figure 4 it can be seen that most of the events occurred during northward IMF or B_z close to zero, consistent with expectations for polar cap aurora (e.g., Berkey et al., 1976). Event 22 (third row of Figure 4), however, occurred during strongly southward IMF, with brief northward turning between 19:15 and 19:45 UT. The corresponding SSUSI images show that the auroral oval is expanded to approximately 70° magnetic latitude, meaning the arcs identified in Event 22 are at a lower latitude than the other events.

Figure 5 shows the current density plots from AMPERE (Anderson et al., 2000, 2014; Waters et al., 2001), solar wind data, and the AL, AU, and SYM-H parameters for the day of Event 22 (14 December). The two panels at the top of Figure 5 show the field-aligned currents from AMPERE at 17:30 UT, around the time of the SSUSI observations shown in Figure 2, in the northern and southern hemispheres. In these panels, the currents are plotted on a magnetic local time grid in a similar manner to the SSUSI images in Figure 2. Red and blue correspond to the upward and downward currents, respectively. The next four panels show midnight/noon and dawn/dusk slices of the field-aligned currents in the northern and southern hemispheres, as a function of time. The bottom four panels show the IMF B_y and B_z components, the solar wind dynamic pressure, the AU and AL indices, and the SYM-H index. It can be seen that an increase in the solar wind pressure (panel 6) is followed by an enhancement in the ring current (indicated by the SYM-H value in the bottom panel of Figure 5). An enhancement in the field-aligned currents measured by AMPERE can also be seen around this time, with an expansion of the auroral oval consistent with the SSUSI images from Figure 2. Furthermore, the arcs identified in the SSUSI images are collocated with the dusk-side R1 current sheet, meaning they are not consistent with being in the polar cap. Therefore, these supporting data show that the arcs identified in the SSUSI images,

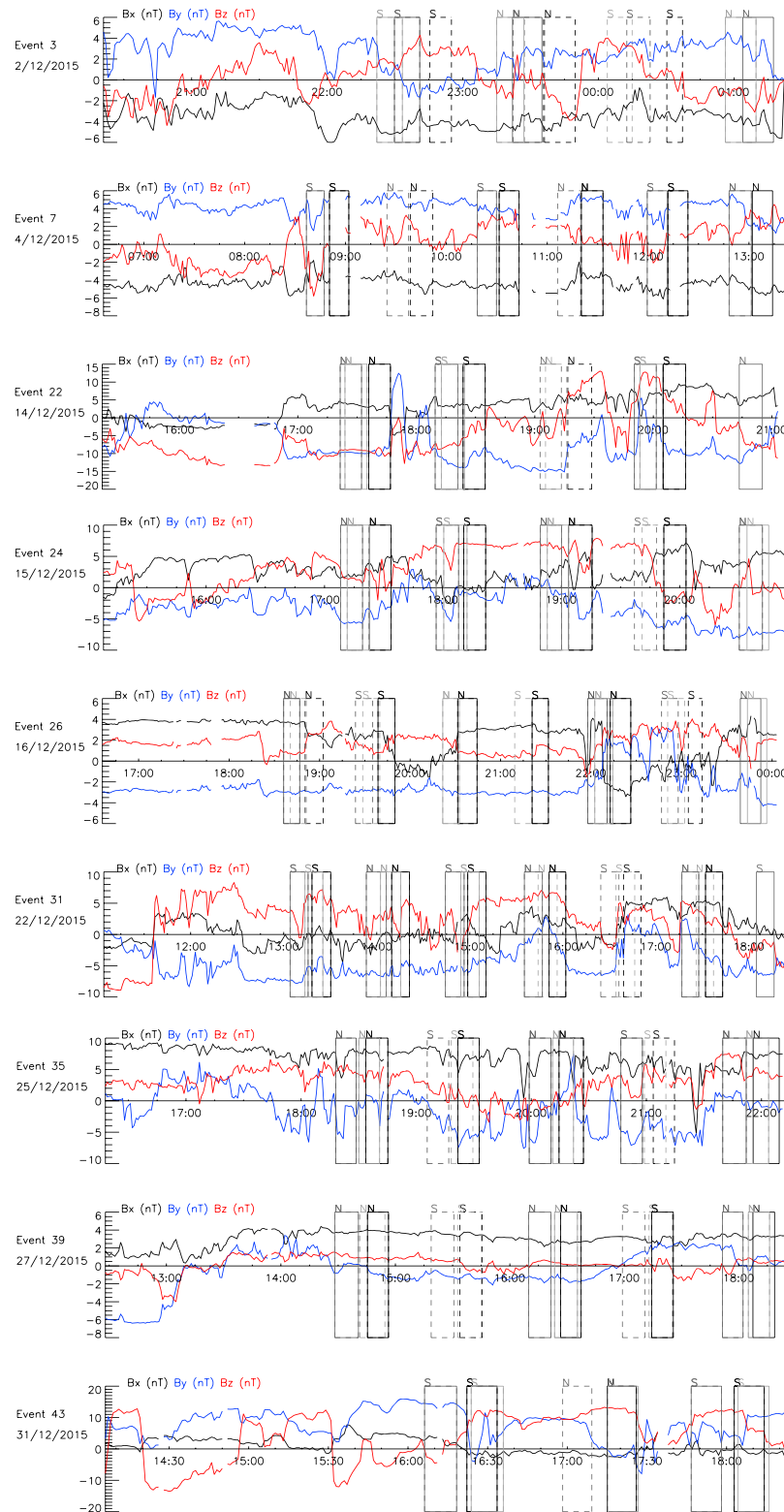


Figure 4. IMF for events where a polar cap arc was seen in both hemispheres, associated with an ion signature. The boxes (as for all these images) show the times of the two Special Sensor Ultraviolet Spectrographic Imager passes. B_x is shown in black, B_y in blue, and B_z in red. The IMF data for Event 3 comes from Artemis with a negligible time lag applied. The rest of the IMF data are from OMNI. Continued overleaf. IMF = interplanetary magnetic field.

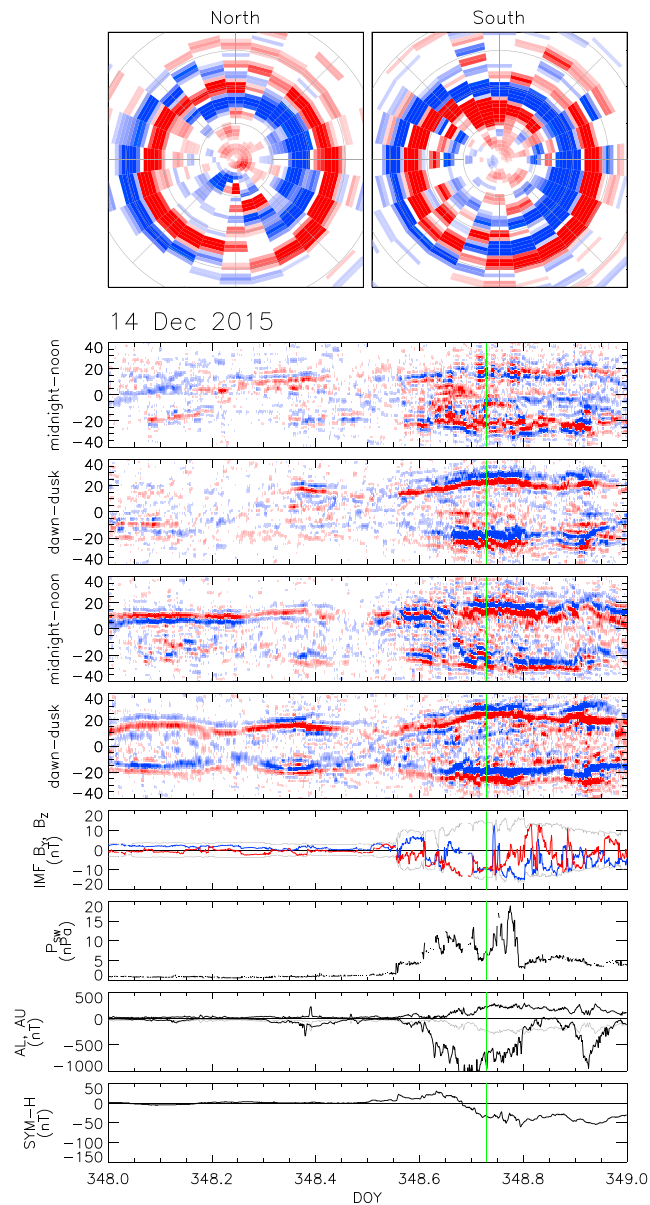


Figure 5. AMPERE, solar wind, and index data for 14 December. The top images show the upward (red) and downward (blue) currents from AMPERE over the northern and southern polar regions at 17:30 UT. This time is indicated in the subsequent plot by the green line. The top four panels of this plot show keograms in the noon-midnight and dawn-dusk meridians of the AMPERE data throughout the day in the northern and southern hemispheres, respectively. The fifth panel shows the interplanetary magnetic field data with the B_z component shown in red and the B_{total} for positive and negative in grey. The next panel shows the solar wind speed in green and the density in pink (between 0 and 20 cm^{-3}). The AL, AU indices are shown in the seventh panel and lastly the SYM-H index in the bottom panel. It can be seen that from approximately 14 UT a geomagnetic storm took place.

although they look similar to PCAs and have similar particle precipitation to other PCA observations, are not PCAs but instead an emission phenomenon associated with a geomagnetic storm.

3.1.2. (b) Consistent with An Open Field Line Mechanism

Figure 6 shows the summary images for Events 11, occurring on 6 December 2015 between 08:17 and 11:41 UT, and 15, 8 December 2015 between 14:25 and 15:18 UT, in the same format as Figure 2. Both of these events have an arc in both hemispheres, each of which is associated with an electron-only signature. In the DMSP SSJ/4 spectrograms, a spike in the electrons that is distinct from the main oval signature is indicated by orange lines; no clear ion signature corresponding to these spikes can be discerned from the ion spectrograms during

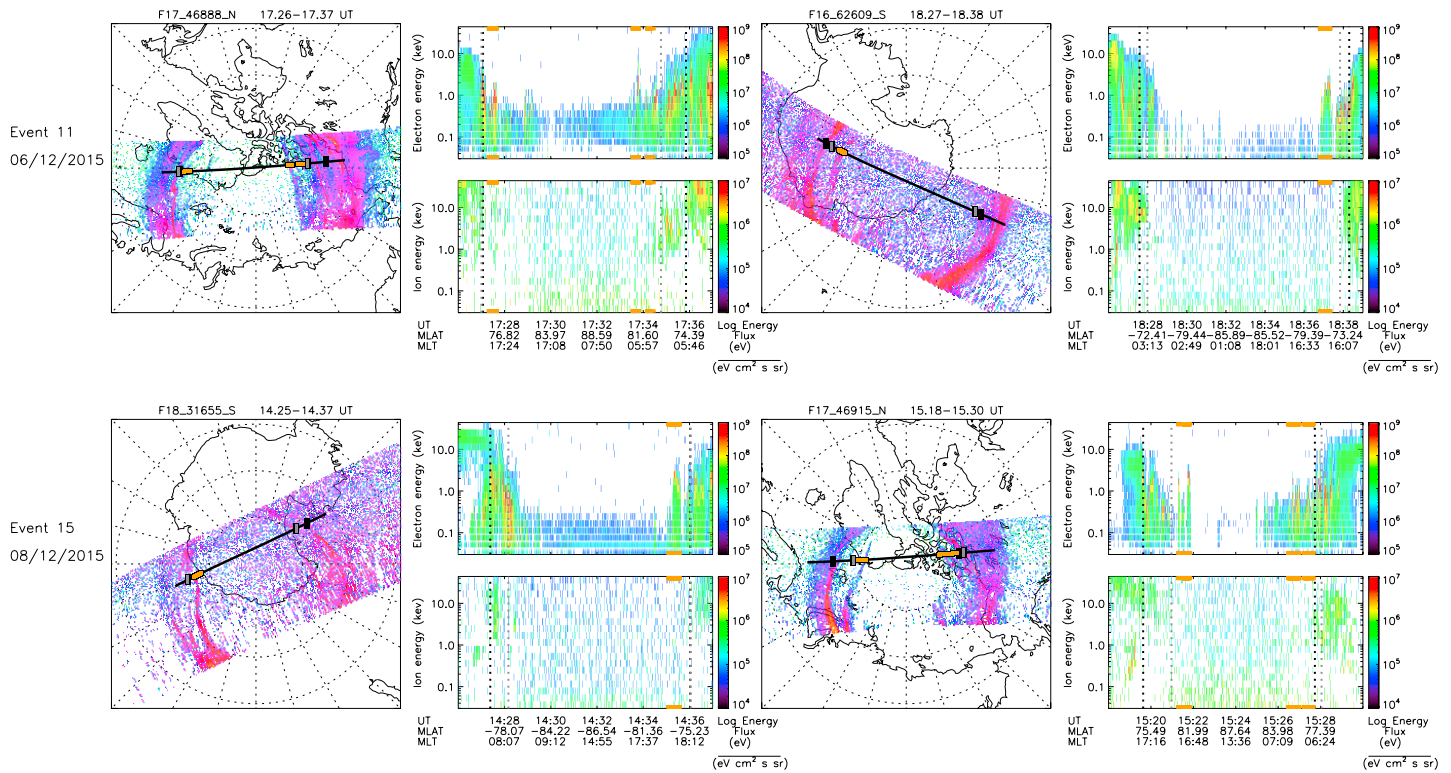


Figure 6. Summary images for events with arcs in both hemispheres associated with electron-only signatures in the same format as Figure 2.

these events. It can be seen in the SSUSI images that each of these electron-only signatures corresponds to a Sun-aligned arc within the polar cap. These features are consistent with what is expected for an open field line mechanism, that is, accelerated polar rain or polar showers (e.g., Newell et al., 2009). However, as these arcs are occurring in both hemispheres at the same time, they are not consistent with polar rain IMF statistics which have a clear hemisphere preference controlled by the IMF B_x component, which in both cases is strongly negative (shown in Figure 7). These events are represented as blue filled circles in Figure 1.

Event 24 (fourth row of Figure 2) shows an example where, as well as the arcs associated with ion signatures observed in both hemispheres, there is an arc in the northern hemisphere pass with an electron-only signature. This event is classified in Table 1 as *both occurring simultaneously* as arcs with different plasma signatures

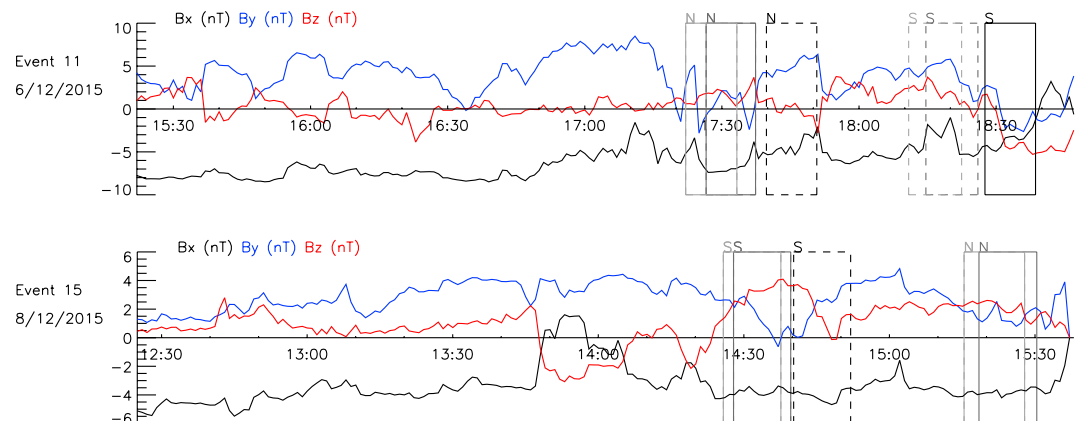


Figure 7. Interplanetary magnetic field for events with electron-only signatures in both hemispheres. The interplanetary magnetic field data for Event 15 comes from Artemis 1 and a time lag of approximately 11 min has been applied.

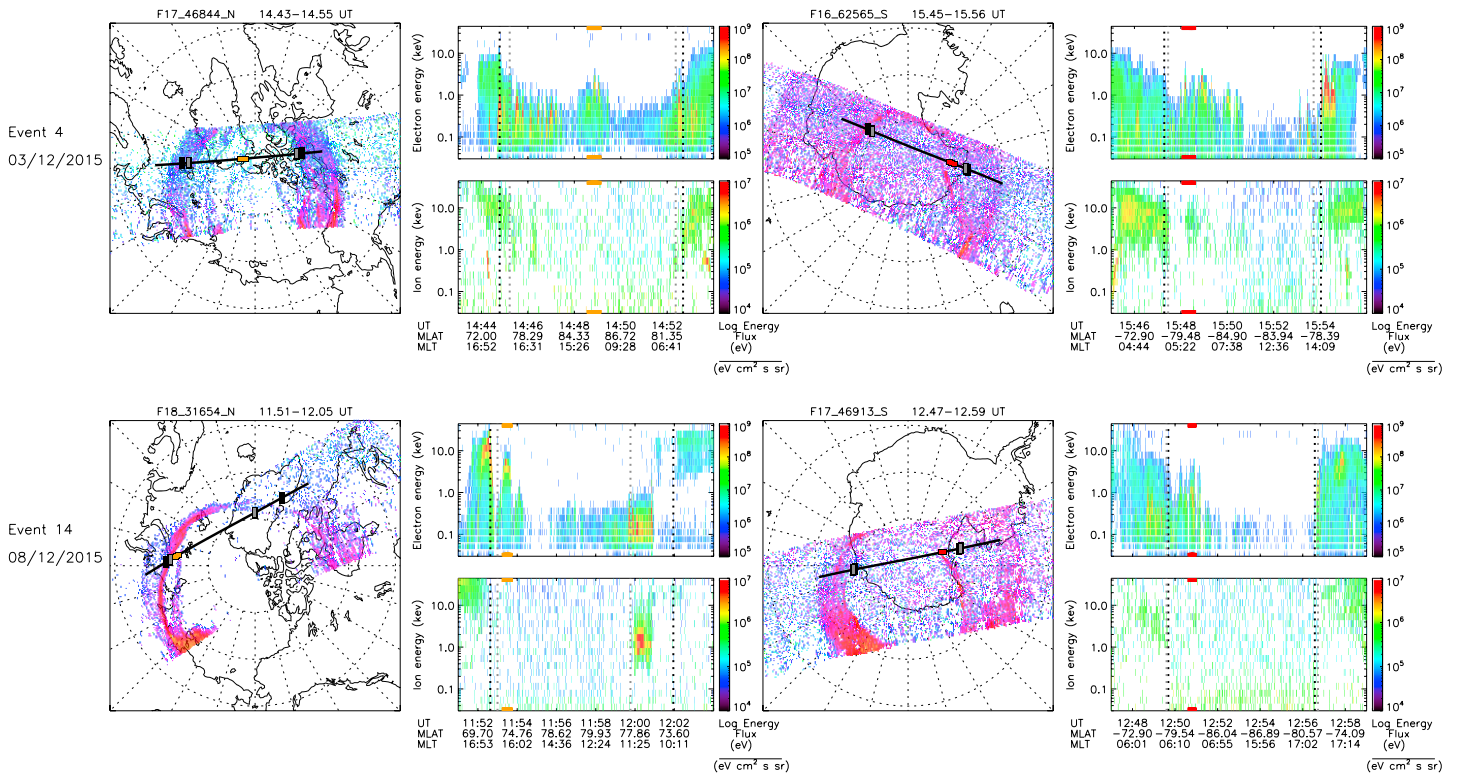


Figure 8. Summary images for events with different signatures in each hemisphere in the same format as Figure 2. The northern hemisphere arc in both of these cases has an electron-only arc and the southern hemisphere contains an arc associated with ion precipitation.

are observed in the same pass. This observation is comparable to Reidy et al. (2017) who found arcs consistent with formation on different magnetic topologies occurring simultaneously.

3.1.3. (c) Not Consistent: Electron-Only Signature in One Hemisphere and an Ion Signature in the Other

Figure 8 shows the summary images for Events 4 and 14 (in the same format as Figure 2) which both have an arc associated with ion precipitation in one hemisphere and an arc associated electron-only signature in the other. The IMF conditions for these events are given in Figure 9. These events are problematic for both closed field line and open field line formation mechanisms and are hence classified as *not consistent* and shown as green solid circles in Figure 1.

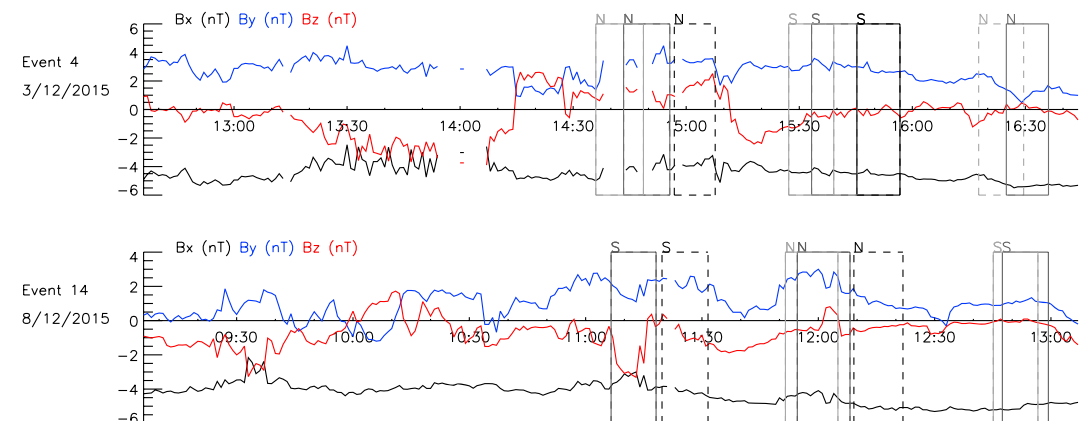


Figure 9. Interplanetary magnetic field conditions for the event with different particle signatures associated with the arcs in each hemisphere.

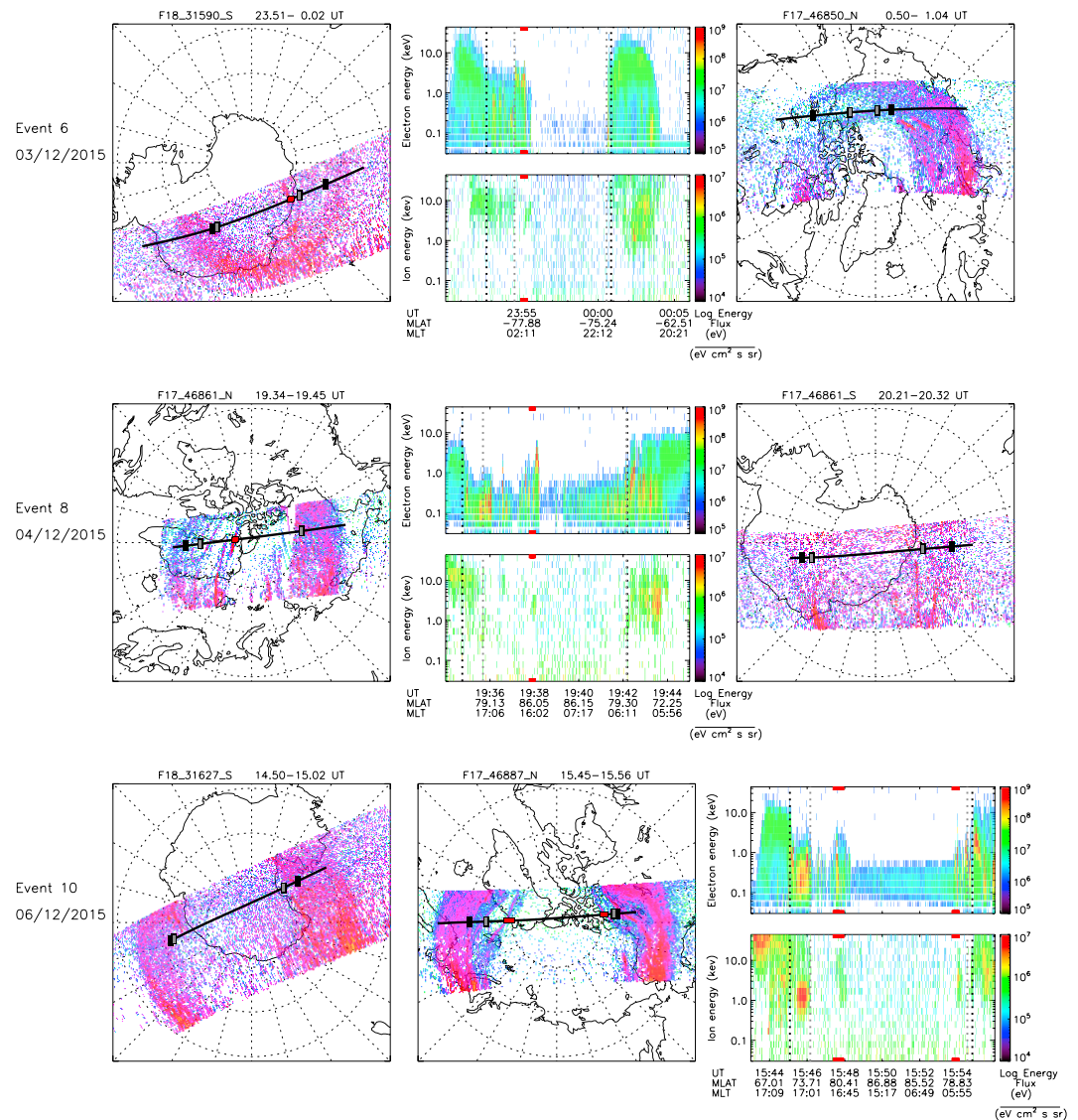


Figure 10. Summary images for events with DMSP SSJ/4 particle data for an arc in only one hemisphere because the footprint misses the arc in the opposite hemisphere. Continued overleaf.

The arcs may be completely unrelated and coincidentally occurring at the same time in opposite hemispheres. The arcs with an electron-only signature, seen in the northern hemisphere for both events, are potentially consistent with an accelerated polar rain formation mechanism. The arcs in the southern hemisphere of both events are associated with ion signatures but do not fit expectations for a closed field line mechanism because they are seen in only one hemisphere. These arcs are possibly examples of nonconjugate theta aurora, which will be discussed further in section 3.2.2, but cannot formally be classified as such as they did not persist for more than one orbit, that is, the arcs were short lived. It could also be the case that the arc giving the ion signature was too short lived to be observed in both hemispheres.

It is possible that these arcs are related, but in that case, it is unclear why the particle precipitation would be different in opposite hemispheres. It could be that the energy flux of the ions in the northern hemisphere are just below detection and, hence we note that there is some uncertainty in the electron-only detections. However, by eye and by applying the semiautomatic method to detect particle signatures described in supplementary material, no clear ion signature corresponding to any of arcs seen in the northern hemisphere SSUSI images can be discerned. Hence, we treat these events as if the arcs are occurring independently but simultaneously in opposite hemispheres.

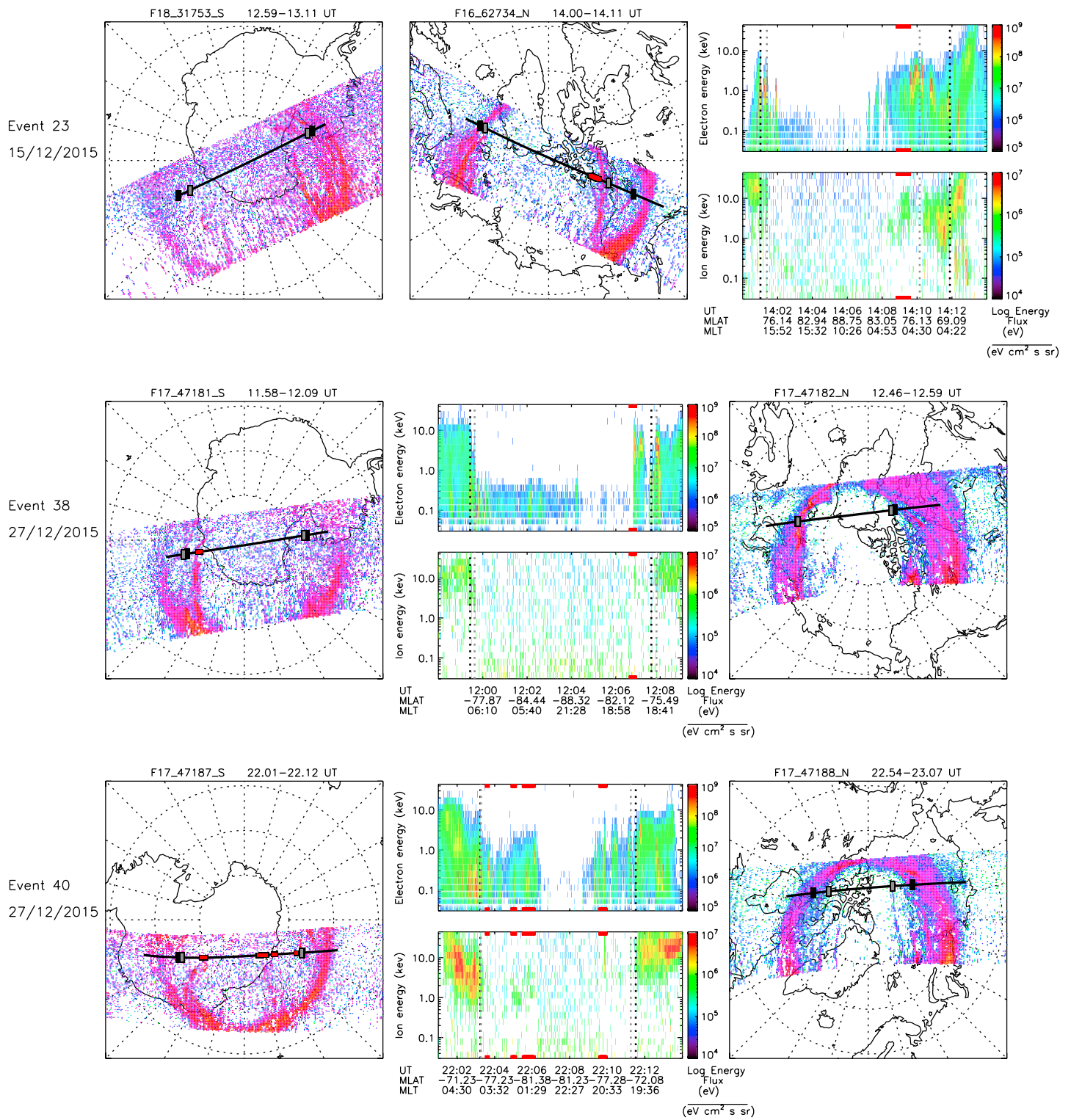


Figure 10. (continued)

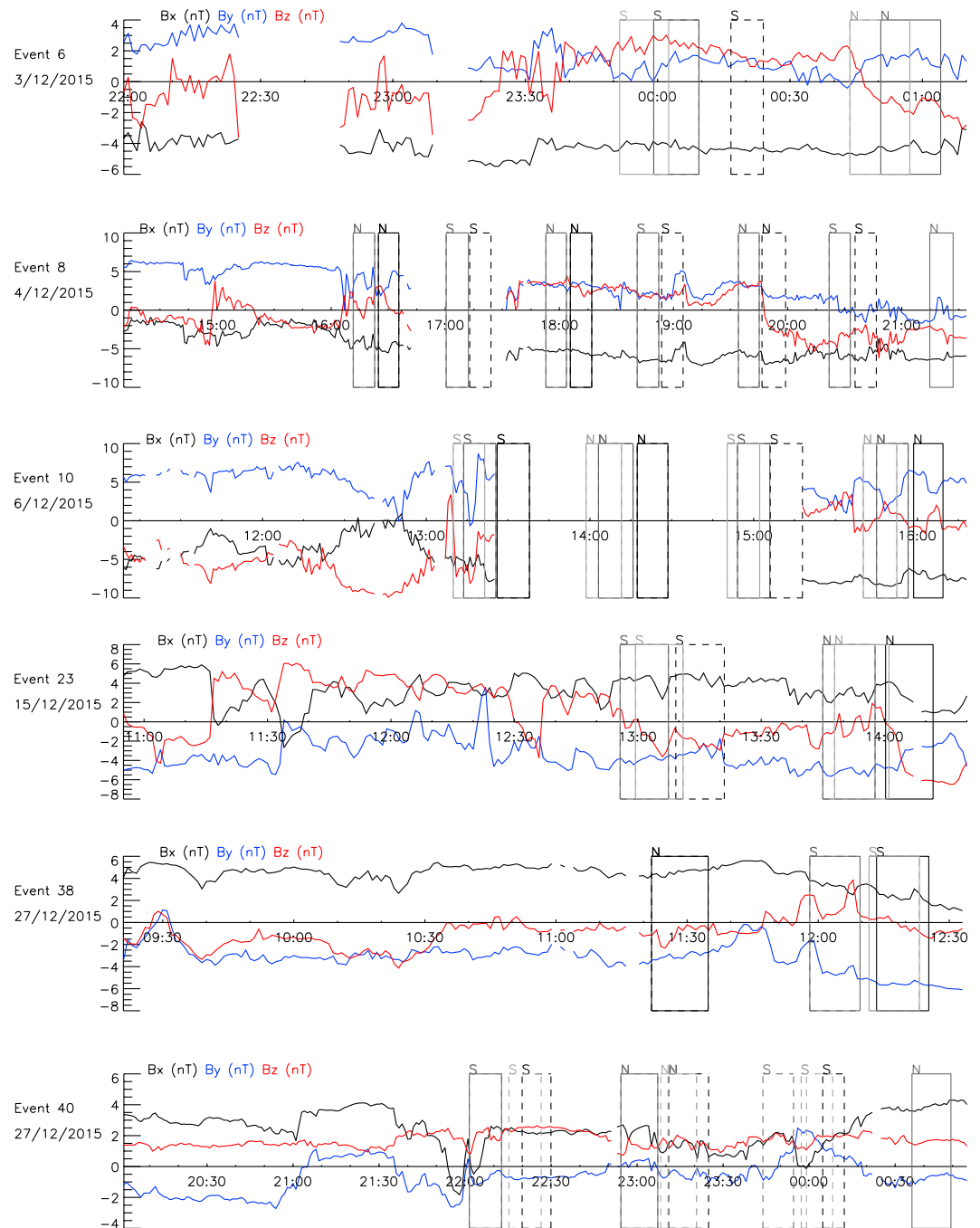


Figure 11. Interplanetary magnetic field plots for events with DMSP data only for arc in one hemisphere. The interplanetary magnetic field data for Event 10 comes from Artemis and a time lag of approximately 8 min has been applied. Continued overleaf.

3.1.4. (d) Potentially Consistent with Closed Field Lines: Particle Data Only Available for an Arc in One of the Hemispheres

The events where the arc intersects a DMSP track in only one hemisphere are shown in Figure 10. As before, the clearest SSUSI image from each hemisphere is shown, with the footprint of the DMSP spacecraft indicated in black. The particle data are shown only for the hemisphere where the arc intersects the DMSP footprint. Figure 11 shows the IMF conditions for each event in the same way as for the other groups. All of the events shown in Figure 10 have an arc associated with an ion signature, and the arc is observed in both hemispheres. Therefore, these events are potentially consistent with a closed field line mechanism (represented as orange

Table 2

Events Identified in SSUSI as Occurring in Only One Hemisphere, Marked with N for North or S for South

Event num.	Start time (UT)	End time	Hem	Ion sig.	Classification
12	07 Dec 2015 17:09	07 Dec 2015 19:05	N	n	Open
16	09 Dec 2015 08:17	09 Dec 2015 11:54	N		
19	11 Dec 2015 10:40	11 Dec 2015 12:19	S		
25	16 Dec 2015 11:49	16 Dec 2015 13:44	N		
30	22 Dec 2015 07:05	22 Dec 2015 10:42	N	y	Not consistent
33	24 Dec 2015 10:03	24 Dec 2015 13:39	N		
34	24 Dec 2015 16:50	24 Dec 2015 18:58	N		
36	26 Dec 2015 06:29	26 Dec 2015 08:24	N		

Note. If the arc intersects the DMSP track, the occurrence of an ion signature is marked with either y or n. The classification of these events is indicated for the arcs with particle data.

filled circles in Figure 1). However, we have seen from Events 4 and 14 (group (c)) that there are cases where the particle signatures are different in the different hemispheres and hence we cannot determine the nature of these arcs with complete certainty.

3.2. Events Occurring in Only One Hemisphere

From surveying SSUSI data from December 2015, eight events were found where a PCA was observed in only one hemisphere. As above, these arcs are analyzed using particle data where the arc intersected the footprint of a DMSP spacecraft. Table 2 lists the date and duration of each event and indicates whether particle data could be obtained for each arc. It can be seen that of these eight events, only two had corresponding particle data. As discussed above, PCAs occurring in only one hemisphere are indicative of an open field line mechanism, and hence electron-only signatures are expected in the particle data, although this is not what we see, as is evident from the final column of Table 2 and discussed below.

3.2.1. Consistent With an Open Field Line Mechanism

Figure 12 shows the one hemisphere event (Event 12) which was associated with an electron-only signature in the northern hemisphere and an "empty" polar cap, that is, no PCA, in the southern hemisphere, although we note that the field of view in the southern hemisphere does not completely show the dawnside of the southern polar cap. This event is represented in Figure 1 as an unfilled blue circle. The algorithm for detecting the plasma signatures has detected three distinct electron-only signatures in the northern hemisphere, two of which, however, are occurring adjacent to the auroral oval; and hence, when talking about the electron-only arc for Event 12, we are referring to the arc on the dawnside that is clearly distinct from the main auroral oval. The electron signature for this arc is similar to those discussed in sections 3.1.2 and 3.1.3 and by Reidy et al. (2017). The IMF conditions for this event (Figure 13) are consistent with polar rain statistics (Yeager & Frank, 1976), that is, the IMF B_x is negative, favoring polar rain in the northern hemisphere, and the IMF B_y is positive which favors polar rain on the dawn side of the northern hemisphere.

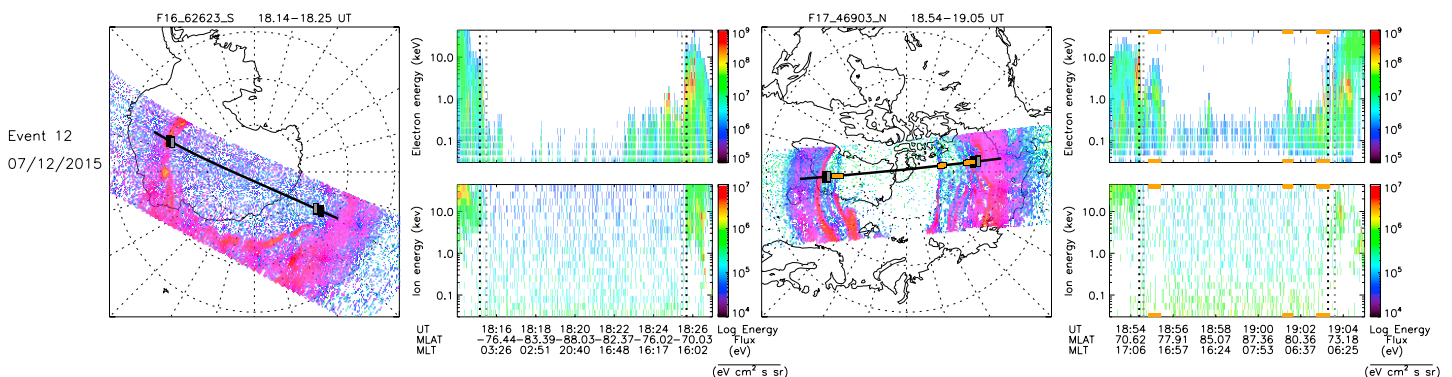


Figure 12. Summary image for event with a polar cap arc in only one hemisphere, associated with an electron-only signature in the same format as Figure 2.

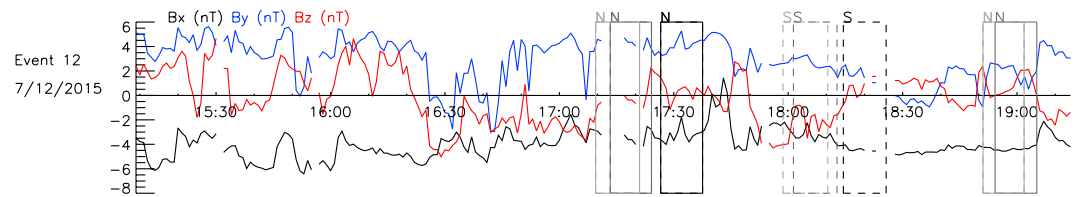


Figure 13. IMF conditions for the one hemisphere electron-only event.

3.2.2. Not Consistent: Nonconjugate Theta Auroras

Figure 14 shows the summary image for Event 30 which occurred on 22 December 2015. A PCA can be seen in the northern hemisphere SSUSI image (between 9:04 and 9:17 UT) that is associated with an ion signature in the corresponding particle data. We note that the DMSPP spacecraft passes quite close to the dayside oval, and hence there is a chance that the ion precipitation may be associated with lobe reconnection; however, the SSUSI image was also examined in the Lyman-alpha channel (not shown) and no obvious sign of a cusp spot was observed. No PCAs are observed in the southern hemisphere SSUSI images and no high energy particle signatures are seen in the corresponding particle data poleward of the auroral oval. A PCA was observed in the subsequent images of the northern hemisphere (not shown), as per the conditions for being classified as one hemisphere event. The combination of an ion signature but presence in only one hemisphere is not consistent with our expectations for either an open field or a closed field line mechanism and hence this event is represented as an unfilled green circle in Figure 1. This observation is similar to that presented by Østgaard et al. (2003) of non-conjugate theta aurora. (The open field line arcs are also strictly nonconjugate but in this paper we take the term to refer specifically to the type of observation reported by Østgaard et al., 2003, in which an ion signature is present or expected to be present, which therefore suggests closed field lines, but which are only seen in one hemisphere).

As a point of interest, we note that in the northern hemisphere SSUSI image (Figure 14), an example of a poleward moving auroral form can be seen between approximately 6 and 10 MLT, which is the auroral signature of a flux transfer event (Fasel, 1995; Milan et al., 2000b; Sandholt & Farrugia, 2007). Phenomenologically, this example is typical of a feature that has been identified as a *bending arc* in some surveys (e.g., Kullen et al., 2002, 2015), but which has been shown to be a signature of dayside reconnection (Carter et al., 2015), as is the case for flux transfer events. Furthermore, this feature is occurring under B_y -dominated conditions, which can be seen in Figure 15 around 09:00 UT, consistent with that found by Kullen et al. (2002, 2015) and Carter et al. (2015).

4. PCA Occurrence Statistics and Seasonal Effects

During this study it was noted, and is evident from the summary images discussed above, that the visibility of PCAs in the southern hemisphere SSUSI images was generally poorer than in the northern hemisphere (e.g., Event 24, fourth row of Figure 2). Furthermore, only one of the 8 one hemisphere events occurred in the southern hemisphere. Hence, we have investigated the seasonal and hemispheric dependence of PCAs and the effect of interspacecraft sensitivity on our observations. Statistics relating to the events discussed above in

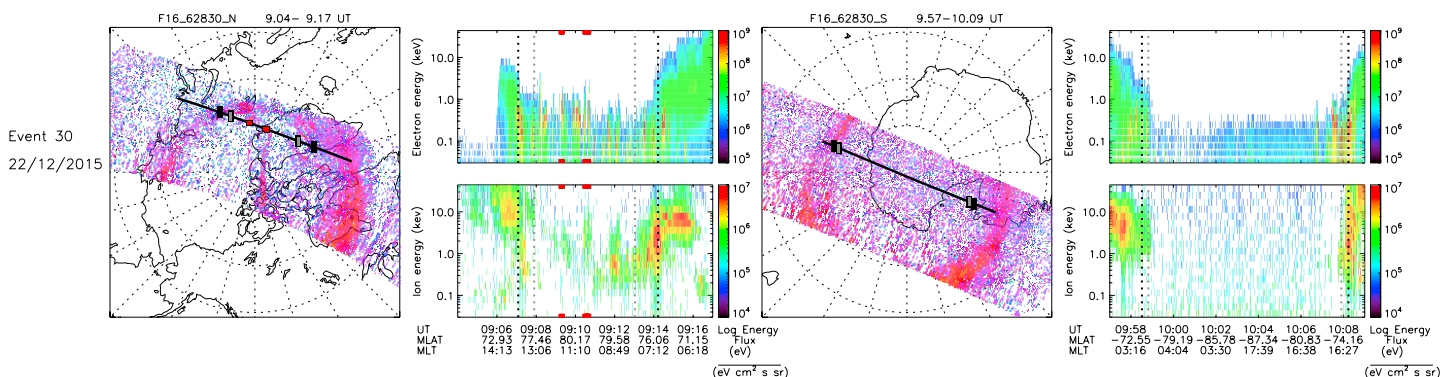


Figure 14. Summary figure for an event containing an arc that appears to be a *non-conjugate* theta aurora, in the same format as Figure 2.

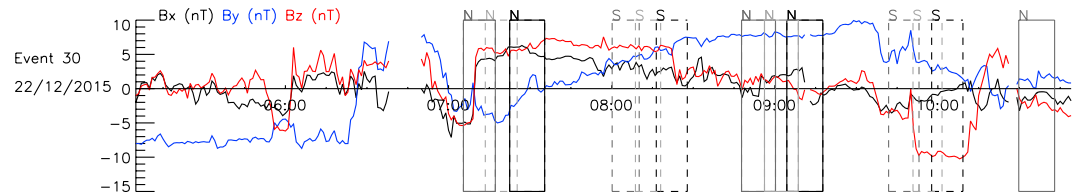


Figure 15. Corresponding interplanetary magnetic field conditions for the *nonconjugate* theta auroras.

December 2015, including a percentage of how many PCAs occurred in each hemisphere, are reported in the right hand column of Table 3. It can be seen that more arcs were recorded in the northern hemisphere than the southern hemisphere, which is expected as a result of the noisier images from the southern hemisphere. To explore this effect further, we examined the SSUSI data from March, June, and September 2015, that is, the equinox months and a month during northern hemisphere summer, and identified PCAs in these months. These results are also presented in Table 3.

It can be seen in Table 3 that the percentages of PCAs recorded in each hemisphere during the equinox months are similar, that is, approximately 40% of the arcs were recorded in the northern hemisphere and approximately 60% in the southern hemisphere for both March and September. The percentage of PCAs seen in each hemisphere for June and December is almost opposite, that is, the hemisphere experiencing summer (South for December and North for June) sees approximately half as many PCAs as in the winter hemisphere. These observations can be explained by sunlight contamination preventing the identification of some features in the summer hemisphere, notwithstanding the attempt to correct for dayglow in the SSUSI data which is undertaken by the SSUSI instrument teams. This observation is consistent with fewer arcs being recorded in the summer hemispheres of June and December. Furthermore, the orbits of the DMSP spacecraft generally occur such that they pass closer to the dayside in the northern hemisphere and closer to the nightside in the southern hemisphere. This means that the northern hemisphere images will generally suffer more from dayglow contamination than the southern hemisphere images, which is hence consistent with the higher number of PCAs observed in the southern hemisphere during the equinox months. (As an additional note: the SSUSI field of view is not equal about the nadir, with more of the swath covering the nightside than the dayside).

Also in Table 3, the percentage of the number of images containing PCAs and the percentage of orbits containing PCAs for each spacecraft are given. It can be seen that, consistently, across all 4 months, more PCAs

Table 3
Statistics from March, June, and December 2015

	March	June	September	December
No. PCA events	50	42	41	43
No. Images with PCA	333	228	327	204
North (%)	41.7	30.7	39.4	67.2
South (%)	58.3	69.3	60.6	32.8
F16 images (%)	11.8	8.0	13.2	7.1
F17 images (%)	20.0	12.0	18.3	11.8
F18 images (%)	7.7	6.4	9.3	6.6
Total images(%)	13.3	8.9	13.5	8.4
F16 orbit (%)	18.9	13.6	21.0	12.0
F17 orbit (%)	29.1	21.7	28.4	21.1
F18 orbit (%)	12.6	11.4	15.2	11.9
Total orbits(%)	20.3	15.5	21.3	14.8

Note. For each month, the total number of PCA events, the total number of images with PCAs, and the percentage of PCAs in each hemisphere are recorded. The percentage of images from each spacecraft which contain PCAs are given in rows 5–7 with a total percentage for all three spacecraft in row 8. The percentage of orbits containing PCAs for each spacecraft, and then as a total of all three are given in rows 9–12. PCA = polar cap arc.

are observed by the SSUSI imager on board DMSP F17. Fewer PCAs are recorded from the SSUSI imager on board DMSP F18, particularly in March, June, and September; this difference is less obvious in December. One potential reason for this difference is that the SSUSI instrument on board DMSP F17 is more sensitive than the other two, (according to the latest SSUSI calibration document by Brian Wolf, private communication, 2017) and hence the weaker PCA events are measured more clearly.

Overall, these surveys show that PCAs are seen by the SSUSI instruments at least 20% of the time. We are likely missing some PCA events due to the effects of the sunlit hemisphere and the field of view of SSUSI due to the DMSP spacecraft orbits.

5. Discussion

In this study we have examined the particle precipitation associated with polar cap arcs and used the ion signature, or lack thereof, to infer the magnetic field topology of these arcs. We have classified the PCA events depending on their hemispheric nature, that is, whether the arcs were seen in one or both hemispheres, using data from the SSUSI instruments on board three of the DMSP spacecraft. These spacecraft are in 90-min Sun-synchronous orbits and hence provide reasonable time resolution for interhemispheric study. From previous PCA studies and proposed mechanisms, arcs occurring in both hemispheres are consistent with a closed field line mechanism, and hence an ion signature is expected in the particle data (e.g., Carter et al., 2017). Arcs seen in only one hemisphere are consistent with an open field line mechanism, and hence an electron-only signature is expected in the particle data (e.g., Newell et al., 2009). In this study, we have defined events as a period of time when PCAs were visible in the SSUSI images rather than by individual PCAs, and hence images containing multiple arcs are classified as one event.

64% of the events were found to contain arcs consistent with a closed field line mechanism (14 events), whereby arcs were seen in both hemispheres and were associated with an ion signature in at least one hemisphere. This percentage includes eight of the nine events from group (a) where an ion signature was detected in both hemispheres (section 3.1.1), also counting Event 24 (fourth row of Figure 2) which also had a separate electron-only arc that was observed to occur simultaneously in the northern hemisphere, and the six events from group (d) where a PCA intersected the footprint of a DMSP spacecraft in only one hemisphere (section 3.1.4). Not included in this statistic from group (a) is Event 22 (third row of Figure 2) which was found to be a misidentified PCA occurring during a geomagnetic storm. As a separate point, it can be seen in Figure 2 that the PCAs identified are (mostly) mirrored about the noon-midnight meridian in the opposite hemispheres. This asymmetry is consistent with previous observations (e.g., Craven et al., 1991) and also consistent with predictions from several mechanisms which place PCAs on closed field lines (e.g., Kullen, 2000; Milan et al., 2005). It can be seen that in the case of Event 22, the arcs are occurring on the same side of the polar cap in both hemispheres, and hence this event does not fit the pattern discussed above.

One of the events identified as being consistent with closed field lines, Event 43 (bottom row of Figure 2) was seen to have an arc in the northern hemisphere with an ion signature detected by one spacecraft orbiting closer to the nightside and an electron-only signature detected by another spacecraft, around the same time, orbiting further sunward (shown in Figure 3). We suggest three possible explanations for this observation. The first is that there is a sensitivity issue with some of the DMSP SSJ/4 instruments (or the ion signatures are sometimes weak) such that ions are not always detected. Second, it could be a spatial feature; the field lines which map further sunward on the arc are those that have most recently been closed; in the Milan et al. (2005) mechanism, after closure, the field lines will seek to contract, but the field lines which map closer to the dayside will contract least. Therefore, it is possible that the precipitating ion signature is less developed. This explanation would imply that an electron-only signature is not a guarantee that the observation occurred on open field lines, which potentially complicates the interpretation of arcs identified as forming by accelerated polar rain. A third explanation for this observation is that the arc may be formed by two independent mechanisms, one on open and the other on closed field lines, each occurring at the same time. Such ideas have been discussed by Eriksson et al. (2005) who suggest PCAs may be formed by two separate dayside and nightside mechanisms. However, it is hard to explain why two independent mechanisms would coincide spatially. A possible explanation may be based on the arguments of Fear et al. (2015), who noted that if a PCA is frozen to a set of magnetic field lines, the flow pattern excited by lobe reconnection will draw the PCA into the cusp. If this applied to both independent mechanisms, it could potentially cause the two elements to align. However, this suggestion is highly speculative, and we reserve further analysis of this to future studies.

27% of the events were seen to contain arcs with an electron-only signature in the DMSP SSJ/4 particle spectrometer (six events): two events with an electron-only arc in both hemispheres (Figure 6), two events with an electron-only arc in one hemisphere and an ion signature arc in the other (Figure 8), one event with an electron-only arc in one hemisphere and nothing in the other (Figure 12), and lastly one event with an electron-only arc occurring simultaneously with an ion signature arc in the northern hemisphere of Event 24 (fourth row of Figure 2). (It is important to note that this percentage and the percentage quoted above for arcs consistent with closed field lines are not additive as both include Event 24).

PCAs associated with an electron-only signature are consistent with an open field line mechanism. Carlson and Cowley (2005) argued that shear flows across open field lines in the magnetotail could accelerate the polar rain enough to generate PCAs. Polar rain favors a hemisphere depending on the IMF B_x component (Yeager & Frank, 1976). Excluding the two events with electron-only arcs in both hemispheres (Events 11 and 15), all of the electron-only arcs identified above occurred in the northern hemisphere and hence, the polar rain statistics would predict the IMF B_x component to be negative during these events. Using IMF data from OMNI, we found that three of the four electron-only arcs observed in only one hemisphere occurred during negative IMF B_x as expected (Event 4, Figure 9; Event 12, Figure 11; and Event 14, Figure 9). However, Event 24 (fourth row of Figure 4) occurred under positive IMF B_x conditions, which is inconsistent with the overall polar rain dependence. Shinohara and Kokubun (1996) found that the occurrence frequency of polar showers without an ion signature (accelerated polar rain) is increased in the northern hemisphere for negative IMF B_x and in the southern hemisphere for positive IMF B_x , but there was a minority of events which did not conform to this trend. Therefore, although the sign of the IMF B_x component makes accelerated polar rain more likely in one hemisphere, it is not impossible in the other. Events 11 and 15 are not included in this discussion as the arcs with electron-only signatures occurred in both hemispheres simultaneously (Figure 6) and hence cannot fit this pattern. It has been reported that an exception to the IMF B_x hemisphere control occurs when there is a closed-loop-flux event in the solar wind (Makita & Meng, 1987). These rare events mean that polar rain will be equally likely in both hemispheres. However, no evidence for this type of event can be seen in the IMF data for Events 11 and 15 (Figure 7). Three out of the six electron-only arcs occurred at the same time as an arc associated with an ion signature; Event 24 where this ion signature arc was seen to occur in both hemisphere and was hence consistent with closed field lines and Events 4 and 14 where the ion signature arc was too short lived to determine its hemispheric nature. These observations are therefore potentially consistent with Reidy et al. (2017) who showed that arcs formed on different topologies could occur at the same time.

An example of a non-conjugate theta aurora, whereby a PCA associated with ion precipitation was observed in only one hemisphere, was given in section 3.2.2. Event 30 (Figure 14) consists of a northern hemisphere arc associated with an ion signature, which by itself would be suggestive of closed field lines, but observations in the southern hemisphere show no counterpart in the SSUSI or DMSP particle data. This type of event is problematic for either an open or a closed field line mechanism and is consistent with that presented by Østgaard et al. (2003, 2007). (The arcs in the southern hemisphere of Events 4 and 14 [Figure 8] are not considered non-conjugate as the arc does not fit the criteria to be classed as a one hemisphere event as it was short lived). One of the possible explanations given by Østgaard et al. (2003) for the absence of the PCA in the empty hemisphere was due to conductivity differences in the summer hemisphere. There have been reports of suppression of discrete auroras in the main oval in the sunlit (summer) hemisphere by Newell et al. (1996); they attributed these observations to an ionospheric feedback mechanism whereby the ionospheric conductance is increased by the precipitation carrying the field-aligned current, which in turn allows the field-aligned current (and hence precipitation) to increase. They argued that this feedback mechanism was less likely to occur in the sunlit ionosphere as the background conductivity is higher. Furthermore, Maes et al. (2015) examined the energy and flux density of accelerated ions above PCAs as a function of solar zenith angle (indicating solar illumination); they found the ions had slightly lower energies above PCAs in the sunlit ionosphere compared with the dark ionosphere, indicative of a decrease in the field-aligned potential drop associated with PCAs in regions of higher ionospheric conductivity. Another explanation for our observations could be the poor data quality in the southern (summer) hemisphere due to the effect of dayglow. The statistical study of data from different seasons (section 4) showed that more arcs were seen in the winter hemispheres than the summer.

By surveying 4 months of SSUSI data, it was found that PCAs are seen by SSUSI at least 20% of the time. More events or images with PCAs are recorded during the equinox months; we attribute this observation to arcs being missed in the summer hemispheres of the other 2 months. PCA events were seen nearly every day during the survey, evenly spread throughout each month. This occurrence frequency is double of what was

reported by Kullen et al. (2002), indicating that SSUSI is potentially more sensitive to the lower energy arcs, perhaps those on open field lines, than Polar UV used by Kullen et al. (2002). However, our value is less than the 40% recorded by Valladares et al. (1994) using ground-based instruments, suggesting SSUSI is not measuring all of the small scale features observed from the ground.

6. Conclusions

This study has used SSUSI and DMSP SSSJ/4 particle data to investigate the formation of PCAs. One month of SSUSI data was surveyed (December 2015) to find PCA events and determine if they were occurring in one or both hemispheres. Particle data from the spectrometer on board the DMSP spacecraft were obtained for the arcs that crossed the spacecraft track to analyse the particle precipitation associated with the arcs and to determine whether they were consistent with an open or closed field line mechanism.

Nine events were found to contain arcs in both hemispheres which were associated with ion precipitation; these arcs are consistent with a closed field line formation mechanism. Six more events were seen to have arcs in both hemispheres but only particle data for an arc in one hemisphere as the arc in the other hemisphere did not cross the footprint of the DMSP spacecraft. These arcs are potentially consistent with a closed field line mechanism, but as some of our both hemisphere events show, we cannot definitively state that there would have been an ion signature if the spacecraft had crossed the arc in the other hemisphere.

Six events were recorded with arcs associated with electron-only precipitation and hence consistent with an open field line mechanism. One of these arcs occurred at the same time (i.e., in the same auroral image) as a closed field line arc and two further events occurred in the opposite hemisphere to a short lived arc associated with an ion signature potentially on closed field lines. These observations suggest that two mechanisms, one on open and the other on closed field lines, can occur simultaneously (Reidy et al., 2017).

An event containing so called nonconjugate theta aurora, whereby an arc associated with an ion signature (which is indicative of closed field lines), was seen in only one hemisphere (which is not indicative of closed field lines) and was discussed. These observations are similar to those presented by Østgaard et al. (2003, 2007). Several suggestions are put forward to explain these observations, including that the SSUSI images in the summer hemisphere are complicated by the effects of daylight. Statistics presented over 4 months during 2015 are supportive of this interpretation. Additionally, it was found that more arcs were detected in the southern hemisphere than the northern hemisphere over the 4 months surveyed in 2015. We suggest that this trend could be due to the orbits of the DMSP spacecraft, which pass closer to the dayside in the northern hemisphere and closer to the nightside in the southern hemisphere, meaning more of the northern hemisphere images suffer the effects of dayglow.

Lastly, the seasonal effect on the occurrence of polar cap aurora was explored using survey results from March, June, September, and December 2015. As discussed above, more arcs were seen in the winter hemisphere of December and June and more PCAs were observed overall during the equinox months, March and September. This observation is attributed to the effects of dayglow on the SSUSI data and hence we conclude PCAs occur at least 20% of the time.

References

- Anderson, B. J., Korth, H., Waters, C. L., Green, D. L., Merkin, V. G., Barnes, R. J., & Dyrud, L. P. (2014). Development of large-scale Birkeland currents determined from the Active Magnetosphere and Planetary Electrodynamics Response Experiment. *Geophysical Research Letters*, *41*, 3017–3025. <https://doi.org/10.1002/2014GL059941>
- Anderson, B. J., Takahashi, K., & Toth, B. A. (2000). Sensing global Birkeland currents with Iridium engineering magnetometer data. *Geophysical Research Letters*, *27*(24), 4045–4048. <https://doi.org/10.1029/2000GL000094>
- Ashrafi, M. (2007). ASK: Auroral structure and kinetics in action. *Astronomy and Geophysics*, *48*(4), 4.35–4.37. <https://doi.org/10.1111/j.1468-4004.2007.48435.x>
- Auster, H. U., Glassmeier, K. H., Magnes, W., Aydogar, O., Baumjohann, W., Constantinescu, D., et al. (2008). The THEMIS fluxgate magnetometer. *Space Science Reviews*, *141*, 235–264. <https://doi.org/10.1007/s11214-008-9365-9>
- Baker, D. N., Bame, S. J., Feldman, W. C., Gosling, J. T., Zwickl, R. D., Slavin, J. A., & Smith, E. J. (1986). Strong electron bidirectional anisotropies in the distant tail - ISEE 3 observations of polar rain. *Journal of Geophysical Research*, *91*, 5637–5662. <https://doi.org/10.1029/JA091iA05p05637>
- Berkey, F. T., Cogger, L. L., Ismail, S., & Kamide, Y. (1976). Evidence for a correlation between Sun-aligned arcs and the interplanetary magnetic field direction. *Geophysical Research Letters*, *3*, 145–147. <https://doi.org/10.1029/GL003i003p00145>
- Carlson, H. C., & Cowley, S. W. H. (2005). Accelerated polar rain electrons as the source of Sun-aligned arcs in the polar cap during northward interplanetary magnetic field conditions. *Journal of Geophysical Research*, *110*, A05302. <https://doi.org/10.1029/2004JA010669>

Acknowledgments

This work was supported by the Natural Environmental Research Council (NERC) studentship number NE/L002531/1. R.C.F. was supported by the United Kingdom's Science and Technology Facilities Council (STFC) Ernest Rutherford Fellowship ST/K004298/2. D.K.W. and B.S.L. are supported by NERC Grant NE/N004051/1. S.E.M. and J.A.C. are supported by the STFC consolidated Grant ST/N000749/1. S.E.M. is also supported by the Research Council of Norway under contract 223252/F50. The SSUSI data were obtained from <http://ssusi.jhuapl.edu/>. The DMSP particle detectors were designed by D. Hardy of Air Force Research Laboratory, and data were obtained from the Johns Hopkins University Applied Physics Laboratory. OMNI and ARTEMIS data were obtained from <https://omniweb.gsfc.nasa.gov/> and <https://sscweb.gsfc.nasa.gov/>, respectively. For the Iridium-derived AMPERE data (<http://ampere.jhuapl.edu/>), we acknowledge the AMPERE Science Center. The authors would also like to thank Stephen Browett and John Coxon for their help during this study.

- Carter, J. A., Milan, S. E., Fear, R. C., Kullen, A., & Hairston, M. R. (2015). Dayside reconnection under interplanetary magnetic field B_y -dominated conditions: The formation and movement of bending arcs. *Journal of Geophysical Research: Space Physics*, *120*, 2967–2978. <https://doi.org/10.1002/2014JA020809>
- Carter, J. A., Milan, S. E., Fear, R. C., Walach, M.-T., Harrison, Z. A., Paxton, L. J., & Hubert, B. (2017). Transpolar arcs observed simultaneously in both hemispheres. *Journal of Geophysical Research: Space Physics*, *122*(6), 6107–6120. <https://doi.org/10.1002/2016JA023830>
- Coxon, J. C., Milan, S. E., & Anderson, B. J. (2018). A Review of Birkeland Current Research using AMPERE, *Electric currents in geospace and beyond, Geophysical Monograph Series* (pp. 259–279) Washington, DC: America Geophysical Union. <https://doi.org/10.1002/9781119324522.ch16>
- Coxon, J. C., Milan, S. E., Carter, J. A., Clausen, L. B. N., Anderson, B. J., & Korth, H. (2016). Seasonal and diurnal variations in AMPERE observations of the Birkeland currents compared to modeled results. *Journal of Geophysical Research: Space Physics*, *121*, 4027–4040. <https://doi.org/10.1002/2015JA022050>
- Coxon, J. C., Milan, S. E., Clausen, L. B. N., Anderson, B. J., & Korth, H. (2014a). The magnitudes of the regions 1 and 2 Birkeland currents observed by AMPERE and their role in solar wind-magnetosphere-ionosphere coupling. *Journal of Geophysical Research: Space Physics*, *119*, 9804–9815. <https://doi.org/10.1002/2014JA020138>
- Coxon, J. C., Milan, S. E., Clausen, L. B. N., Anderson, B. J., & Korth, H. (2014b). A superposed epoch analysis of the regions 1 and 2 Birkeland currents observed by AMPERE during substorms. *Journal of Geophysical Research: Space Physics*, *119*, 9834–9846. <https://doi.org/10.1002/2014JA020500>
- Craven, J. D., Murphree, J. S., Cogger, L. L., & Frank, L. A. (1991). Simultaneous optical observations of transpolar arcs in the two polar caps. *Geophysical Research Letters*, *18*, 2297–2300. <https://doi.org/10.1029/91GL02308>
- Cumnock, J. A., Blomberg, L. G., Kullen, A., Karlsson, T., & Sundberg, K. Å. T. (2009). Small-scale characteristics of extremely high latitude aurora. *Annales Geophysicae*, *27*, 3335–3347. <https://doi.org/10.5194/angeo-27-3335-2009>
- Dahlgren, H., Ivchenko, N., Sullivan, J., Lanchester, B. S., Marklund, G., & Whiter, D. (2008). Morphology and dynamics of aurora at fine scale: First results from the ASK instrument. *Annales de Geophysique*, *26*, 1041–1048. <https://doi.org/10.5194/angeo-26-1041-2008>
- Eriksson, S., Baker, J. B. H., Petrinc, S. M., Wang, H., Rich, F. J., Kuznetsova, M., et al. (2005). On the generation of enhanced sunward convection and transpolar aurora in the high-latitude ionosphere by magnetic merging. *Journal of Geophysical Research*, *110*, A11218. <https://doi.org/10.1029/2005JA011149>
- Fasel, G. J. (1995). Dayside poleward moving auroral forms: A statistical study. *Journal of Geophysical Research*, *100*, 11,891–11,905. <https://doi.org/10.1029/95JA00854>
- Fear, R. C., & Milan, S. E. (2012a). The IMF dependence of the local time of transpolar arcs: Implications for formation mechanism. *Journal of Geophysical Research*, *117*, A03213. <https://doi.org/10.1029/2011JA017209>
- Fear, R. C., & Milan, S. E. (2012b). Ionospheric flows relating to transpolar arc formation. *Journal of Geophysical Research*, *117*, A09230. <https://doi.org/10.1029/2012JA017830>
- Fear, R. C., Milan, S. E., Carter, J. A., & Maggiolo, R. (2015). The interaction between transpolar arcs and cusp spots. *Geophysical Research Letters*, *42*, 9685–9693. <https://doi.org/10.1002/2015GL066194>
- Fear, R. C., Milan, S. E., Maggiolo, R., Fazakerley, A. N., Dandouras, I., & Mende, S. B. (2014). Direct observation of closed magnetic flux trapped in the high-latitude magnetosphere. *Science*, *346*, 1506–1510. <https://doi.org/10.1126/science.1257377>
- Frank, L. A., Craven, J. D., Burch, J. L., & Winningham, J. D. (1982). Polar views of the Earth's aurora with dynamics explorer. *Geophysical Research Letters*, *9*, 1001–1004. <https://doi.org/10.1029/GL009i009p01001>
- Frank, L. A., Craven, J. D., Gurnett, D. A., Shawhan, S. D., Burch, J. L., Winningham, J. D., et al. (1986). The theta aurora. *Journal of Geophysical Research*, *91*, 3177–3224. <https://doi.org/10.1029/JA091iA03p03177>
- Frey, H. U., Mende, S. B., Fuselier, S. A., Immel, T. J., & Østgaard, N. (2003). Proton aurora in the cusp during southward IMF. *Journal of Geophysical Research*, *108*, 1277. <https://doi.org/10.1029/2003JA009861>
- Goudarzi, A., Lester, M., Milan, S. E., & Frey, H. U. (2008). Multi-instrumentation observations of a transpolar arc in the northern hemisphere. *Annales Geophysicae*, *26*, 201–210. <https://doi.org/10.5194/angeo-26-201-2008>
- Gussenhoven, M. S. (1982). Extremely high latitude auroras. *Journal of Geophysical Research*, *87*, 2401–2412. <https://doi.org/10.1029/JA087iA04p02401>
- Gussenhoven, M. S., Hardy, D. A., Heinemann, N., & Burkhardt, R. K. (1984). Morphology of the polar rain. *Journal of Geophysical Research*, *89*, 9785–9800. <https://doi.org/10.1029/JA089iA11p09785>
- Hardy, D. A. (1984). Intense fluxes of low-energy electrons at geomagnetic latitudes above 85°. *Journal of Geophysical Research*, *89*, 3883–3892. <https://doi.org/10.1029/JA089iA06p03883>
- Hardy, D. A., Burke, W. J., & Gussenhoven, M. S. (1982). DMSP optical and electron measurements in the vicinity of polar cap arcs. *Journal of Geophysical Research*, *87*, 2413–2430. <https://doi.org/10.1029/JA087iA04p02413>
- Hardy, D. A., Gussenhoven, M. S., Riehl, K., Burkhardt, R., Heinemann, N., & Schumaker, T. (1986). The Characteristics of polar cap precipitation and their dependence on the interplanetary magnetic field and the solar wind. In Y. Kamide & J. A. Slavin (Eds.), *Solar wind magnetosphere coupling, astrophysics and space science library* (Vol. 126, pp. 575–604). Dordrecht, Netherlands: D. Reidel Publishing Co. https://doi.org/10.1007/978-90-277-2303-1_40
- Hosokawa, K., Moen, J. I., Shiokawa, K., & Otsuka, Y. (2011). Motion of polar cap arcs. *Journal of Geophysical Research*, *116*, A01305. <https://doi.org/10.1029/2010JA015906>
- King, J. H., & Papitashvili, N. E. (2005). Solar wind spatial scales in and comparisons of hourly Wind and ACE plasma and magnetic field data. *Journal of Geophysical Research*, *110*, A02104. <https://doi.org/10.1029/2004JA010649>
- Kullen, A. (2000). The connection between transpolar arcs and magnetotail rotation. *Geophysical Research Letters*, *27*, 73–76. <https://doi.org/10.1029/1999GL010675>
- Kullen, A., Brittnacher, M., Cumnock, J. A., & Blomberg, L. G. (2002). Solar wind dependence of the occurrence and motion of polar auroral arcs: A statistical study. *Journal of Geophysical Research*, *107*, 1362. <https://doi.org/10.1029/2002JA009245>
- Kullen, A., Fear, R. C., Milan, S. E., Carter, J. A., & Karlsson, T. (2015). The statistical difference between bending arcs and regular polar arcs. *Journal of Geophysical Research: Space Physics*, *120*, 10. <https://doi.org/10.1002/2015JA021298>
- Maes, L., Maggiolo, R., De Keyser, J., Dandouras, I., Fear, R. C., Fontaine, D., & Haaland, S. (2015). Solar illumination control of ionospheric outflow above polar cap arcs. *Journal of Geophysical Research*, *42*, 1304–1311. <https://doi.org/10.1002/2014GL062972>
- Maggiolo, R., Echim, M., de Keyser, J., Fontaine, D., Jacquy, C., & Dandouras, I. (2011). Polar cap ion beams during periods of northward IMF: Cluster statistical results. *Annales Geophysicae*, *29*, 771–787. <https://doi.org/10.5194/angeo-29-771-2011>
- Makita, K., & Meng, C.-I. (1987). Long-period polar rain variations, solar wind and hemispherically symmetric polar rain. *Journal of Geophysical Research*, *92*, 7381–7393. <https://doi.org/10.1029/JA092iA07p07381>

- Mawson, D. (1916). Auroral observations at the Cape Royds station, Antarctica. *Transactions of The Royal Society of South Australia*, *XL*, 151–212.
- Meng, C.-I., & Kroehl, H. W. (1977). Intense uniform precipitation of low-energy electrons over the polar cap. *Journal of Geophysical Research*, *82*, 2305–2313. <https://doi.org/10.1029/JA082i016p02305>
- Milan, S. E., Hubert, B., & Grocott, A. (2005). Formation and motion of a transpolar arc in response to dayside and nightside reconnection. *Journal of Geophysical Research*, *110*, A01212. <https://doi.org/10.1029/2004JA010835>
- Milan, S. E., Lester, M., Cowley, S. W. H., & Brittnacher, M. (2000a). Dayside convection and auroral morphology during an interval of northward interplanetary magnetic field. *Annales Geophysicae*, *18*, 436–444. <https://doi.org/10.1007/s00585-000-0436-9>
- Milan, S. E., Lester, M., Cowley, S. W. H., & Brittnacher, M. (2000b). Convection and auroral response to a southward turning of the IMF: Polar UVI, CUTLASS, and IMAGE signatures of transient magnetic flux transfer at the magnetopause. *Journal of Geophysical Research*, *105*, 15,741–15,756. <https://doi.org/10.1029/2000JA900022>
- Newell, P. T., Liou, K., & Wilson, G. R. (2009). Polar cap particle precipitation and aurora: Review and commentary. *Journal of Atmospheric and Solar-Terrestrial Physics*, *71*, 199–215. <https://doi.org/10.1016/j.jastp.2008.11.004>
- Newell, P. T., Meng, C.-I., & Lyons, K. M. (1996). Suppression of discrete aurorae by sunlight. *Nature*, *381*, 766–767. <https://doi.org/10.1038/381766a0>
- Østgaard, N., Mende, S. B., Frey, H. U., Frank, L. A., & Sigwarth, J. B. (2003). Observations of non-conjugate theta aurora. *Geophysical Research Letters*, *30*, 2125. <https://doi.org/10.1029/2003GL017914>
- Østgaard, N., Mende, S. B., Frey, H. U., Sigwarth, J. B., Åsnes, A., & Weygand, J. M. (2007). Auroral conjugacy studies based on global imaging. *Journal of Atmospheric and Solar-Terrestrial Physics*, *69*, 249–255. <https://doi.org/10.1016/j.jastp.2006.05.026>
- Paxton, L. J., Morrison, D., Zhang, Y., Kil, H., Wolven, B., Ogorzalek, B. S., et al. (2002). Validation of Remote Sensing Products Produced by the Special Sensor Ultraviolet Scanning Imager (SSUSI): A far UV-Imaging Spectrograph on DMSP F-16. In A. M. Larar & M. G. Mlynczak (Eds.), *Optical spectroscopic techniques, remote sensing, and instrumentation for atmospheric and space research IV, Proc. SPIE 4485* (Vol. 4485, pp. 338–348). San Diego, CA: SPIE. <https://doi.org/10.1117/12.454268>
- Reidy, J. A., Fear, R. C., Whiter, D. K., Lanchester, B. S., Kavanagh, A. J., Paxton, L. J., et al. (2017). Multi-instrument observation of simultaneous polar cap auroras on open and closed magnetic field lines. *Journal of Geophysical Research: Space Physics*, *122*, 4367–4386. <https://doi.org/10.1002/2016JA023718>
- Sandholt, P. E., & Farrugia, C. J. (2007). Poleward moving auroral forms (PMAFs) revisited: Responses of aurorae, plasma convection and Birkeland currents in the pre- and postnoon sectors under positive and negative IMF B_y conditions. *Annales Geophysicae*, *25*, 1629–1652. <https://doi.org/10.5194/angeo-25-1629-2007>
- Shinohara, I., & Kokubun, S. (1996). Statistical properties of particle precipitation in the polar cap during intervals of northward interplanetary magnetic field. *Journal of Geophysical Research*, *101*, 69–82. <https://doi.org/10.1029/95JA01848>
- Shue, J.-H., Newell, P. T., Liou, K., & Meng, C.-I. (2001). The quantitative relationship between auroral brightness and solar EUV pedersen conductance. *Journal of Geophysical Research*, *106*, 5883–5894. <https://doi.org/10.1029/2000JA003002>
- Valladares, C. E., Carlson, H. C. Jr., & Fukui, K. (1994). Interplanetary magnetic field dependency of stable Sun-aligned polar cap arcs. *Journal of Geophysical Research*, *99*, 6247–6272. <https://doi.org/10.1029/93JA03255>
- Waters, C. L., Anderson, B. J., & Liou, K. (2001). Estimation of global field-aligned currents using the Iridium system magnetometer data. *Geophysical Research Letters*, *28*(11), 2165–2168. <https://doi.org/10.1029/2000GL012725>
- Winningham, J. D., & Heikkila, W. J. (1974). Polar cap auroral electron fluxes observed with ISIS 1. *Journal of Geophysical Research*, *79*, 949. <https://doi.org/10.1029/JA079i007p00949>
- Xing, J., Zhang, Q., Han, D., Zhang, Y., Sato, N., Zhang, S., et al. (2018). Conjugate observations of the evolution of polar cap arcs in both hemispheres. *Journal of Geophysical Research: Space Physics*, *123*, 1794–1805. <https://doi.org/10.1002/2017JA024272>
- Yeager, D. Y., & Frank, L. A. (1976). Low-energy electron intensities at large distances over the Earth's polar cap. *Journal of Geophysical Research*, *81*, 3966–3976. <https://doi.org/10.1029/JA081i022p03966>
- Yeoman, T. K., Lester, M., Cowley, S. W. H., Milan, S. E., Moen, J., & Sandholt, P. E. (1997). Simultaneous observations of the cusp in optical, DMSP and HF radar data. *Geophysical Research Letters*, *24*, 2251–2254. <https://doi.org/10.1029/97GL02072>
- Zhu, L., Schunk, R. W., & Sojka, J. J. (1997). Polar cap arcs: A review. *Journal of Atmospheric and Solar Terrestrial Physics*, *59*, 1087–1126. [https://doi.org/10.1016/S1364-6826\(96\)00113-7](https://doi.org/10.1016/S1364-6826(96)00113-7)